HHS Public Access

Author manuscript

Cortex. Author manuscript; available in PMC 2021 March 29.

Published in final edited form as:

Cortex. 2017 July ; 92: 119–138. doi:10.1016/j.cortex.2017.03.016.

Resting-state functional reorganization in Parkinson's disease: An activation likelihood estimation meta-analysis

Masoud Tahmasian[a,b,c,e,*], **Simon B. Eickhoff**[f,g,h], **Kathrin Giehl**[b], **Frank Schwartz**[a], **Damian M. Herz**[i,j], **Alexander Drzezga**[b], **Thilo van Eimeren**[a,b], **Angela R. Laird**[k], **Peter T. Fox**[l,m], **Habibolah Khazaie**[e], **Mojtaba Zarei**[c,d], **Carsten Eggers**[a,n], **Claudia R. Eickhoff**[g,o]

[a]Department of Neurology, University Hospital Cologne, Germany

[b]Department of Nuclear Medicine, University Hospital Cologne, Cologne, Germany

[c]Institute of Medical Sciences and Technology, Shahid Beheshti University, Tehran, Iran

[d]School of Cognitive Sciences, Institute for Research in Fundamental Sciences (IPM), Tehran, Iran

[e]Sleep Disorders Research Center, Kermanshah University of Medical Sciences (KUMS), Kermanshah, Iran

[f]Institute of Clinical Neuroscience & Medical Psychology, Heinrich Heine University Düsseldorf, Düsseldorf, Germany

[g]Institute for Systems Neuroscience, Medical Faculty, Heinrich-Heine University Düsseldorf, Germany

[h]Institute of Neuroscience and Medicine (INM-1, INM-7), Research Center Jülich, Jülich, Germany

[i]Medical Research Council Brain Network Dynamics Unit at the University of Oxford, Oxford, United Kingdom

[j]Nuffield Department of Clinical Neurosciences, University of Oxford, John Radcliffe Hospital, Oxford, United Kingdom

[k]Department of Physics, Florida International University, Miami, FL, USA

[l]Research Imaging Institute, University of Texas Health Science Center, San Antonio, TX, USA

[m]South Texas Veterans Health Care System, San Antonio, TX, USA

[n]Department of Neurology, Phillips University Marburg, Germany

[*]*Corresponding author*. Institute of Medical Science and Technology, Shahid Beheshti University, Daneshjou Boulevard, Velenjak, P.O. Box 1983969411, Tehran, Iran. masoudtahmasian@gmail.com (M. Tahmasian).

Conflict of interest statement

The authors declare that the research was conducted in the absence of any commercial or financial relationships that could be construed as a potential conflict of interest.

Supplementary data

Supplementary data related to this article can be found at http://dx.doi.org/10.1016/j.cortex.2017.03.016.

[o]Department of Psychiatry, Psychotherapy, and Psychosomatics, RWTH Aachen University, Aachen, Germany

Abstract

Parkinson's disease (PD) is a common progressive neurodegenerative disorder. Studies using resting-state functional magnetic resonance imaging (fMRI) to investigate underlying pathophysiology of motor and non-motor symptoms in PD yielded largely inconsistent results. This quantitative neuroimaging meta-analysis aims to identify consistent abnormal intrinsic functional patterns in PD across studies. We used PubMed to retrieve suitable resting-state studies and stereotactic data were extracted from 28 individual between-group comparisons. Convergence across their findings was tested using the activation likelihood estimation (ALE) approach. We found convergent evidence for intrinsic functional disturbances in bilateral inferior parietal lobule (IPL) and the supramarginal gyrus in PD patients compared to healthy subjects. In follow-up task-based and task-independent functional connectivity (FC) analyses using two independent healthy subject data sets, we found that the regions showing convergent aberrations in PD formed an interconnected network mainly with the default mode network (DMN). Behavioral characterization of these regions using the BrainMap database suggested associated dysfunction of perception and executive processes. Taken together, our findings highlight the role of parietal cortex in the pathophysiology of PD.

Keywords

Resting-state fMRI; ALE meta-analysis; Inferior parietal lobule; Default mode network

1. Introduction

Parkinson's disease (PD) is a common progressive neurodegenerative disorder, which affects more than seven million people globally (Willis, 2013; de Lau & Breteler, 2006). It has been demonstrated that functional and structural loss of dopaminergic neurons in the substantia nigra pars compacta (SNc) leads to fundamental alterations in basal ganglia circuits. Involvement of cortical and subcortical brain areas and other neurotransmitter changes (e.g., cholinergic or serotonergic systems), however, also contribute substantially to PD symptoms (Braak, Ghebremedhin, Rub, Bratzke, & Del Tredici, 2004; Del Tredici, Rub, De Vos, Bohl, & Braak, 2002). PD is clinically characterized by progressive motor features such as bradykinesia, rigidity, resting tremor and postural instability (Braak et al., 2003; Jankovic, 2008). In addition, several studies highlighted the relevance of non-motor symptoms including depression, cognitive impairment, anxiety, sleep disorders, and impulsive behavior in PD (Chaudhuri, Healy, Schapira, & National Institute for Clinical, 2006). These symptoms are contributing to a severe disability and inevitably lead to a decreased quality of life of PD patients. However, their neuroanatomical and neurochemical substrates are still poorly understood.

To assess the neural correlates of motor and non-motor symptoms in PD, numerous functional neuroimaging studies localized and quantified abnormalities within and between different brain regions (cf. Eckert, Tang, & Eidelberg, 2007; Prodoehl, Burciu, &

Vaillancourt, 2014; Stoessl, 2009; Tahmasian, Bettray, et al., 2015). Task-based functional magnetic resonance imaging (fMRI) has been used in many studies over the last two decades to assess aberrant recruitment of brain regions in the context of experimental paradigms using a subtraction approach between a target and a control condition (Herz, Eickhoff, Lokkegaard, & Siebner, 2014; Rana, Masroor, & Khan, 2013; Rottschy, Kleiman, et al., 2013). However, these task-based designs are strongly influenced by compliance and task performance of subjects, which might have confounded the results.

As an alternative approach, resting state fMRI (rs-fMRI) has been widely applied over the last decade in healthy populations and various neurodegenerative and neuropsychiatric disorders (Biswal, 2012; Khazaie et al., 2017; Klupp et al., 2015; Meng et al., 2014; Pasquini et al., 2014; Riedl et al., 2014; Seeley, Crawford, Zhou, Miller, & Greicius, 2009; Tahmasian et al., 2013; Tahmasian, Pasquini, et al., 2015; Tahmasian et al., 2016). Rs-fMRI is based on fluctuations of the blood-oxygen-level dependent (BOLD) signal that are associated with the intrinsic neuronal activity of the brain, while subjects are in the awake state without performing any specific task, i.e., in an endogenously controlled state of mind-wandering (Biswal, 2012; Fox, Snyder, et al., 2005; Snyder & Raichle, 2012). In contrast to task-related fMRI, rs-fMRI substantially reduces the potential influences of compliance and task performance (Di Martino et al., 2008). There is a rich literature evaluating intrinsic functional disturbances in PD using different rs-fMRI analysis methods, including seed-based functional connectivity (FC), independent component analysis (ICA), regional homogeneity (ReHo), amplitude of low frequency oscillations (ALFF), and graph analysis under different medication states (for review see: Prodoehl et al., 2014; Tahmasian, Bettray, et al., 2015).

Previously, we summarized the current rs-fMRI literature in PD and suggested that seed-based FC and effective connectivity are valuable techniques for assessing the disruption of connectivity between specific brain areas, while network-based and graph analysis methods are promising approaches for assessing functional alterations across the whole brain. ReHo and ALFF can also be applied to study local intrinsic abnormalities in PD. In addition, we concluded that dopamine replacement therapy induces functional reorganization of the brain and normalizes functional alterations in PD (Tahmasian, Bettray, et al., 2015). Despite abovementioned advantages, the previous rs-fMRI studies point to diverse and often conflicting findings. One reason for this predicament seems to be the variety of rs-fMRI preprocessing (e.g., different normalization, motion correction, and global signal regression) and analyzing strategies. Seed-based methods measure FC between the averaged BOLD time course of a region of interest (ROI) (or a seed) and the time course of other brain voxels; ICA is a data-driven approach that identifies intrinsic neural networks; ALFF, as a regional approach, assesses the regional intensity of oscillatory fluctuations in the BOLD signal; ReHo is also a regional method, which calculates the similarity between the BOLD signal of particular voxels and the nearest voxels within a given cluster. Thus, ReHo and ALFF are conceptually different pertaining to connectivity because they investigate local phenomena. The link between the different aspects of resting state physiology is still not clarified yet. Thus, in order to characterize resting state abnormalities in PD as comprehensively as possible we included findings from all approaches. Of note, we excluded seed-based FC studies because such analyses entail a strong prior selection-bias in

the seed-definition, which limits their findings to functionally connected areas rather than looking at the whole brain level. Graph analysis evaluates properties of brain nodes connected by edges to identify the topological organization of brain networks (Biswal, 2012; Lee, Smyser, & Shimony, 2013). In addition, there is a large heterogeneity across studies in terms of clinical stage, medication, and PD-related clinical variability including different motor subtypes (e.g., tremor-dominant, akinetic-rigid, levodopa-induced dyskinesia, freezing of gait), cognitive deficits (e.g., mild cognitive impairment, dementia), or non-motor symptoms (e.g., hallucinations, depression, hypomania, impulsivity, and REM sleep behavior disorder) (Tahmasian, Bettray, et al., 2015). Taken together, this diversity has strongly contributed to provide an ambiguous picture of pathophysiological mechanisms underlying PD. Hence, a consolidation of this literature is needed to overcome the diversity and inconsistencies of previously published work, which is characterized by small sample sizes, clinical heterogeneity and analytic inconsistencies.

Activation likelihood estimation (ALE) has recently developed as a powerful method for coordinate-based meta-analyses (CBMA), providing a synoptic view of distributed neuroimaging findings. This method gives the unique opportunity to draw statistical inference on the convergence of previous neuroimaging findings across different methods in a quantitative way. Specifically, CBMA tests “where” in the brain the convergence between reported coordinates is higher than expected by chance (Eickhoff & Bzdok, 2013; Eickhoff, Bzdok, Laird, Kurth, & Fox, 2012; Laird, Eickhoff, Kurth, et al., 2009; Turkeltaub, Eden, Jones, & Zeffiro, 2002). Here, we applied an ALE meta-analysis on reported functional resting-state data derived from comparison between patients with PD and healthy controls to provide an assessment of convergent functional disturbance across published rs-fMRI studies in PD.

2. Methods

2.1. Data source and study selection

Based on the Preferred Reporting Items for Systematic Reviews and Meta-Analyses (PRISMA) statement (Moher, Liberati, Tetzlaff, Altman, & Group, 2009), we conducted our search on PubMed database in October 2015 and by reference tracing of the retrieved articles. Our search strings were: (Parkinson’s disease OR Parkinson disease) AND (resting state fMRI OR FC in resting state functional magnetic resonance), which resulted in 107 studies. Three additional studies were included through review papers and reference tracing (Fig. 1, Table 1). We included English peer-reviewed papers that used resting-state fMRI to compare a sample of PD patients with healthy controls. Furthermore, case-reports, letters to editors, meta-analysis, or review studies that report no original data, studies that did not report whole-brain analysis, methodological papers, studies which did not report standard space coordinates, intervention studies, studies, which focused only on a group of PD patients, and studies with a sample size of 7 or less subjects in each group were excluded.

2.2. Data extraction

Data was extracted by two independent investigators (M.T and F.S). Recorded data includes the first author’s name, year of publication, age, gender, number of subjects, the analysis

approach (ALFF, ICA, ReHo, graph-theory), and the peak coordinates (x,y,z) in Talairach (Talairach & Tournoux, 1988) or Montreal Neurological Institute (MNI) (Evans et al., 1993) stereotactic space. Coordinates reported in Talairach space were transformed into MNI space for analysis (Lancaster et al., 2007). The extracted stereotactic coordinates were used for conducting the ALE meta-analysis. If a study did not report the coordinates of activation maxima explicitly, we contacted the authors. One should note that here, "study" reflects an individual scientific paper and "experiment" represents a single analysis or contrast of interest in a given study yielding localization information (i.e., PD > Controls or PD < Controls). We also excluded studies that analyzed a previously published dataset.

Although during the last decade, studies using seed-based FC analysis expanded our current understanding regarding the neural basis of PD, we excluded them to avoid biased findings. In ALE approach, significant convergent voxels across all experiments, which are above the random distribution across the whole brain are detected. However, including seed-based FC analyses refract the assumption that each voxel has the a priori same chance of being activated and therefore leads to inflated significance for the respective regions. Thus, to avoid such bias and self-fulfilling prophecies, it is proposed to only include results of whole-brain analyses in neuroimaging meta-analyses (Eickhoff, Laird, Fox, Lancaster, & Fox, 2017; Muller et al., 2016).

2.3. ALE

We used the revised version of ALE (Eickhoff et al., 2012) as implemented in MATLAB to conduct the statistical analysis (Eickhoff et al., 2012; Eickhoff et al., 2009; Turkeltaub et al., 2012). ALE tests the significant convergence between activation foci from different experiments (e.g., PD > controls, PD < controls) relative to a null-hypothesis of random spatial association. In the first step, the ALE algorithm models the reported foci as center peaks of 3D Gaussian probability distributions, which reflect the spatial uncertainty associated with each focus. The uncertainty arises from "between-subject variations" e.g., different neuroanatomy and small sample sizes and "between-laboratory variance" e.g., different brain templates and normalization strategies. The number of participants in the smaller group of each experiment determines the width of the spatial uncertainty of any focus (Eickhoff et al., 2009; Turkeltaub et al., 2002). In the second step, the probability distributions of all activation foci in a particular experiment are combined for each voxel, which creates a modeled activation (MA) map for that particular experiment (Turkeltaub et al., 2012). The final ALE map was then computed as the union of these MA maps and described the convergence of findings across all experiments. Subsequently, in the third step, an analytical approach based on non-linear histogram integration is performed to test against the null hypothesis of random spatial association. Our statistical threshold for significance was $p < .05$ cluster level family-wise error (cFWE) corrected (Eickhoff & Bzdok, 2013; Eickhoff et al., 2017). Moreover, in order to identify convergent regional versus long-distance functional alterations, we performed supplementary analyses across different rs-fMRI approaches.

2.4. Task-based FC: meta-analytic connectivity modeling

Using the regions identified in the above ALE meta-analysis as seeds, we then performed meta-analytic co-activation modeling (MACM) in order to delineate brain areas, which are significantly co-activated with these. The MACM approach determines brain regions that co-activate with a seed region across numerous neuroimaging experiments at a level above chance (Eickhoff et al., 2011; Robinson, Laird, Glahn, Lovallo, & Fox, 2010). We used the BrainMap database that includes coordinates of reported activation foci as well as the associated meta-data of more than 10,000 neuroimaging experiments (Laird et al., 2011; Laird, Eickhoff, Kurth, et al., 2009; Turner & Laird, 2012). In detail, we identified all experiments in the BrainMap database, which show activation in at least one voxel of the seed regions. Subsequently, we conducted quantitative meta-analysis to test for convergence across the foci reported in the experiments. Significant convergence of reported foci in the seeds and other brain areas represents consistent co-activation of other voxels with our seeds. In general, MACM thus yields functional interactions of cortical modules based on their whole-brain co-activation patterns (Eickhoff et al., 2011; Laird et al., 2013).

2.5. Task-independent FC: resting-state

In addition to the MACM analysis, we also conducted whole-brain resting-state FC analysis, again using the regions determined in our ALE meta-analysis as seeds, in order to identify task-independent patterns of functionally connected brain regions. We used rs-fMRI data of 124 healthy individuals (40 males and 84 females, age, 46.56 ± 17.56 years). This data was collected by the Nathan Kline Institute (‘Rockland’ sample’; Nooner et al., 2012) and shared as part of the “International Neuroimaging Data sharing Initiative” (INDI, http://fcon_1000.projects.nitrc.org/indi/pro/nki.html).

Images were obtained on a Siemens TrioTim 3T scanner using BOLD contrast [gradient-echo echo planar imaging (EPI) pulse sequence, repetition time (TR) = 2.5 sec, echo time (TE) = 30 msec, flip angle = 80°, in-plane resolution = 3.0 × 3.0 mm, 38 axial slices (3.0 mm thickness), covering the entire brain]. After removing the first four scans, we used SPM8 (www.fil.ion.ucl.ac.uk/spm) for preprocessing and analysis of images. We applied head motion correction, spatial normalized to the MNI single subject template using the ‘unified segmentation’ approach, and smoothing by a 5-mm FWHM Gaussian kernel. Subsequently, the six motion parameters derived from the image realignment, the first derivative of the realignment parameters, the averaged white matter, and CSF signal were considered as nuisance variables in both first-order and second-order models. Afterwards, we applied a low-frequency band-pass filter (.01 and .08 Hz).

In the next step, time courses for all voxels of a given seed were extracted and then we calculated Pearson correlation coefficients between the averaged time course of each seed and that of all other voxels in the brain to calculate FC. The resulting voxel-wise correlation coefficients were transformed into Fisher’s Z-scores and tested for consistency across subjects. Results were corrected for multiple comparisons using cFWE-correction at $p < .05$ as described previously (Goodkind et al., 2015).

2.6. Behavioral decoding

In order to assess the behavioral roles of the seed regions determined in our ALE meta-analysis, we performed behavioral decoding using the BrainMap database. Behavioral domains of this database include major categories i.e., cognition, action, perception, emotion, and interoception, and their related sub-categories (Fox, Laird, et al., 2005; Fox, Snyder, et al., 2005) (see http://www.brainmap.org/scribe). In detail, the behavioral profile was identified by detecting the taxonomic labels for which the probability of finding activation in the seed regions identified in the main ALE analysis was significantly higher than by chance across the whole BrainMap database (Laird, Eickhoff, Kurth, et al., 2009; Laird, Eickhoff, Li, et al., 2009; Rottschy, Caspers, et al., 2013). Significant level was set as $p < .05$ using a binomial test (Caspers et al., 2014; Muller, Cieslik, Laird, Fox, & Eickhoff, 2013; Rottschy, Caspers, et al., 2013).

3. Results

Twenty-eight publications that recruited 701 unique subjects were included (Amboni et al., 2014; Baggio et al., 2014; Borroni et al., 2015; Chen et al., 2015; Choe, Yeo, Chung, Kim, & Lim, 2013; Esposito et al., 2013; Gorges et al., 2015; Gottlich et al., 2013; Hou, Wu, Hallett, Chan, & Wu, 2014; Hu et al., 2015; Kwak et al., 2012; Luo et al., 2014; Madhyastha et al., 2015; Onu, Badea, Roceanu, Tivarus, & Bajenaru, 2015; Sheng et al., 2014; Skidmore et al., 2013; Szewczyk-Krolikowski et al., 2014; Tan et al., 2015; Tessitore et al., 2012; Tinaz, Lauro, Hallett, & Horovitz, 2015; Wei et al., 2014; Wen, Wu, Liu, Li, & Yao, 2013; Wu et al., 2009, 2015; Yang et al., 2013; Yao et al., 2014; Zhang et al., 2013, 2015) (Table 1, Fig. 1).

Here, we tested for significant convergence across the rs-fMRI findings, pooling across different rs-fMRI analyses in order to provide a global assessment of aberrant functional patterns in PD patients. These publications collectively reported results from 63 experiments of which 20 experiments were reported as “PD-OFF < Controls” contrasts, 18 experiments as “PD-OFF > Controls” contrasts, 14 experiments as “PD-ON < Controls” contrasts, 11 experiments as the “PD-ON > Controls” contrasts, and 10 experiments as the “PD-ON<>PD-OFF”.

3.1. Convergence of rs-fMRI findings in PD

Testing for significant convergence across all rs-fMRI experiments comparing PD patients to healthy controls yielded a significant cluster in the posterior part of right inferior parietal lobule (IPL) ($p < .05$ cFWE, 136 voxels) (Fig. 2A). The cluster of convergence in the right IPL was mainly (64.5%) driven by “PD-OFF > Controls” experiments with additional 32.5% from “PD-ON < Controls” contrasts. Importantly, there was a substantial contribution from different methodologies, as ALFF studies contributed 18%, ReHo 46.5% and ICA 35.5%. Eleven experiments from six studies contributed to this finding (Amboni et al., 2014; Gorges et al., 2015; Onu et al., 2015; Tessitore et al., 2012; Wen et al., 2013; Zhang et al., 2015), one of them focused on PD patients with and without depression (Wen et al., 2013) and two of them compared normal and cognitively impaired PD patients (Amboni et al., 2014; Gorges et al., 2015). The identified cluster in the posterior part of right IPL (local maximum:

48/ −62/34 in MNI space) was anatomically allocated using the SPM Anatomy Toolbox (Eickhoff et al., 2005) to PGp (a caudal area of IPL) (50.1%) and PGa (a rostral area of IPL) (27.8%) defined by histological criteria (Caspers et al., 2008; Caspers et al., 2006) (Fig. 2A).

Further analyses demonstrated that PD patients showed a consistent functional increase in two regions compared to healthy controls: (*i*) the posterior part of right IPL (local maximum: 48/ −62/36 in MNI space, 107 voxels) allocated to PGa (40.1%) and PGp (30.6%). Here ALFF studies contributed 25.5%, ReHo 72.5% and ICA 2%. The cluster of convergence in the right IPL was mainly driven by contribution from “PD-OFF > Controls” (98%) and six experiments from three studies (Gorges et al., 2015; Wen et al., 2013; Zhang et al., 2015), while two of them focused on non-motor symptoms of PD (Gorges et al., 2015; Wen et al., 2013); (*ii*) the posterior part of left IPL. This cluster was located in areas PGa (66.7%), PFm (6.3%), and PGp (5%) (local maximum: −42/ −66/42 in MNI space, 173 voxels). The convergence cluster in the left IPL was mainly (78%) driven by “PD-OFF > Controls” contrasts with additional contribution (22%) from “PD-ON > Controls” contrasts and eight experiments from six studies (Choe et al., 2013; Gorges et al., 2015; Hu et al., 2015; Wen et al., 2013; Yang et al., 2013; Zhang et al., 2015), while two of them focused on non-motor symptoms of PD (Gorges et al., 2015; Wen et al., 2013). Here ALFF studies contributed 9.5%, ReHo 74.5% and ICA 16% (Fig. 2B).

In order to evaluate the effects of medications, supplementary analyses targeting convergence among different medication states were performed. The analysis of “PD-OFF < Controls” yielded no significant findings. In turn, for the “PD-OFF > Controls” condition, we found increased functional parameters in three regions: (*i*) the right supramarginal gyrus/ temporoparietal junction (TPJ) (local maximum: 62/ −34/32 in MNI space, 84 voxels, cf. Bzdok, Langner, Schilbach, Jakobs, et al., 2013; Krall, et al., 2015). Of the cluster’s volume 72.3% was located in area PF, 22.2% in area PFcm, and 3.3% in area PFt (Caspers et al., 2008; Caspers et al., 2006). ALFF studies contributed 26%, ReHo 49% and ICA 25% to this cluster from four studies (Onu et al., 2015; Wu et al., 2015; Yang et al., 2013; Zhang et al., 2015); (*ii*) The posterior part of right IPL (local maximum: 48/ −62/36 in MNI space, 128 voxels). Cluster maxima were located in areas PGa (39.3%) and PGp (31.5%). ALFF studies contributed 26.5% and ReHo 73.5%, while ICA and graph-theoretical experiments did not contribute to the cluster from two studies (Wen et al., 2013; Zhang et al., 2015); (*iii*) The posterior part of left IPL extending into area PGa (56.1%) and area PGp (7.8%) (local maximum: −40/ −68/42 in MNI space, 139 voxels). Here ALFF studies contributed 17.5%, ReHo 82.5 from three studies (Choe et al., 2013; Wen et al., 2013; Zhang et al., 2015) (Fig. 2C). Only one study that contributed for the “PD-OFF > Controls” condition assessed the non-motor symptoms of PD (Wen et al., 2013).

In the “PD-ON < Controls” contrast, we found significant convergence in the posterior part of right IPL (local maximum: 46/ −64/26 in MNI space 112 voxels). This cluster was located in areas PGp (52.5%) and PGa (4.6%) (Fig. 2D) and completely driven by three ICA studies (Amboni et al., 2014; Gorges et al., 2015; Tessitore et al., 2012), from which two studies assessed cognitive impairment in PD patients (Amboni et al., 2014; Gorges et al., 2015). In turn there was no significant convergence across the “PD-ON > Controls” contrasts. Due to

the low number of available experiments in the “PD-OFF” versus “PD-ON ” contrasts, no reliable meta-analyses could be conducted with these contrasts.

Supplementary analyses assessing converging results from regional (i.e., ALFF and ReHo) versus long distance connectivity (i.e., ICA and Graph) confirmed the key findings. Yuan and colleagues demonstrated that ALFF and ReHo are positively correlated, which suggests that increased spontaneous neuronal activity in the neighboring voxels is associated with higher amplitude fluctuations of the rs-fMRI signal (Yuan et al., 2013). While combing the ALFF and ReHo studies, the “PD > Controls” contrast showed the left IPL (local maximum: −40/ −68/42 in MNI space, 157 voxels), the right IPL (local maximum: 48/ −62/36 in MNI space 123 voxels), and the left middle temporal gyrus (local maximum: −58/ −24/ −11 in MNI space 104 voxels). On the other hand, the “PD < Controls” contrast showed the cerebellar vermis (local maximum: −2/ −56/ −4 in MNI space, 99 voxels) (Supplement Fig. 1A). The three studies using graph approach performed their analyses on a voxel-wise whole-brain approach and calculated strength, degree, betweenness centrality, clustering coefficient and local efficiency as the measurements of FC, functional integration and segregation. Hence, strength or degree is expected to be correlated with connectivity as measured in the ICA approach. Thus, we combined graph and ICA studies and found significant convergent area in the right IPL (local maximum: 48/ −63/26 in MNI space 118 voxels) in the “PD < Controls” contrast (Supplement Fig. 1B). There was no significant finding in the “PD > Controls” contrast. All of these findings were based on $p < .05$ cFWE. We also performed ALE analyses for each individual rs-fMRI method, but there were not enough data to provide significant results. In summary, the performed series of quantitative meta-analyses on rs-fMRI findings in PD patients revealed consistent evidence of abnormal regions mainly in the posterior part of IPL.

3.2. Task-based FC patterns

In order to map brain regions that feature significant coactivation with the seed regions identified by the ALE meta-analysis, we performed a MACM analysis. This analysis indicated significant ($p < .05$ cFWE corrected) co-activation of our seeds with several regions. The posterior part of right IPL, which showed convergence across all experiments comparing all PD patients to healthy controls showed significant FC with the posterior part of left IPL (PGa, PGp, Pfm), IPS, TPJ (Bzdok, Langner, Schilbach, Jakobs, et al., 2013; Caspers et al., 2006, 2008; Krall et al., 2015; Rottschy, Caspers, et al., 2013), precuneus and posterior cingulate cortex (PCC) (Bzdok et al., 2015), mid-cingulate cortex (Hoffstaedter et al., 2014), middle and superior frontal gyrus, and orbitofrontal gyrus (Bzdok, Langner, Schilbach, Engemann, et al., 2013; Rottschy, Caspers, et al., 2013) (Fig. 3A).

The regions showing convergence in “PD > Controls” (i.e., the posterior part of right and left IPL) featured significant task-based co-activations with the bilateral IPL (PGa, PGp, Pfm), supramarginal gyrus/TPJ, precuneus and posterior cingulate cortex (PCC), mid-cingulate cortex, middle and superior frontal gyri, orbitofrontal gyrus, posterior-medial frontal cortex (Bzdok et al., 2015; Nachev, Kennard, & Husain, 2008), precentral (Eickhoff et al., 2006), left middle temporal gyrus (Krall et al., 2015), left insula (Kurth, Zilles, Fox, Laird, & Eickhoff, 2010), left amygdala and hippocampus (Robinson et al., 2010, 2015) (Fig. 3B).

Regions showing convergence in “PD-OFF > Controls” condition demonstrated significant connectivity with several other areas. (*i*) the right supramarginal gyrus connected to bilateral IPL (Pfcm, PFt), posterior-medial frontal cortex, bilateral insula, bilateral inferior frontal gyrus (IFG) (Amunts et al., 1999; Costafreda et al., 2006), bilateral thalamus (Behrens et al., 2003), and precentral gyrus; (*i*) the right IPL connected to the left IPL (PGa, PGp, Pfm), mid-cingulate cortex, and precuneus; (*iii*) the left IPL connected to right IPL (PGa, PGp), left insula, left IFG, and posterior-medial frontal cortex (Fig. 3C).

The posterior part of right IPL, which showed convergent “PD-ON < Controls” revealed significant connectivity with left IPL (PGa, PGp, Pfm),mid-cingulate cortex, and precuneus (Fig. 3D).

3.3. Task-independent FC patterns

Here, we identified patterns of task-independent (resting-state) FC patterns across the whole brain for each of the consistent seed regions determined in our ALE meta-analysis. The findings demonstrated that the posterior part of right IPL significantly connected with the left IPL, bilateral middle and superior frontal gyri, mid-cingulate cortex, precuneus, middle and inferior temporal gyri, cerebellum, hippocampus, IFG, orbitofrontal cortex, and caudate nucleus. Moreover, the left IPL had similar FC patterns (Fig. 4A and B).

Among areas, which showed common higher FC in PD patients in the OFF-state compared to healthy controls, the right supramarginal gyrus connected to bilateral IPL (Pfcm, PFt), bilateral middle and superior frontal gyri, mid-cingulate cortex, insula, thalamus, middle occipital gyrus, middle and inferior temporal gyri, cerebellum, parahippocampus and IFG. In addition, the right IPL and the left IPL connected to contralateral IPL, bilateral middle and superior frontal gyri, mid-cingulate cortex, precuneus, middle and inferior temporal gyri, cerebellum, hippocampus, IFG, orbitofrontal cortex, and caudate nucleus (Fig. 4C). A similar FC pattern was observed for the posterior part of right IPL as a convergent lower FC in PD patients in the ON-state compared to healthy subjects (Fig. 4D).

3.4. Convergent findings between task-based and task-independent FC

Conjunction analyses across the MACMs and resting-state FC maps were computed to delineate the consensus connectivity (cf Amft et al., 2015; Clos, Rottschy, Laird, Fox, & Eickhoff, 2014). of the seeds. In detail, the posterior part of right IPL connected to the posterior part of left IPL, bilateral middle and superior frontal gyri, mid-cingulate cortex, precuneus, and orbitofrontal cortex. The left IPL connected to the right IPL, bilateral middle and superior frontal gyri, precental gyrus, posterior-medial frontal cortex, mid-cingulate cortex, precuneus, PCC, insula, hippocampus and orbitofrontal cortex. The right supramarginal gyrus showed consistent FC with bilateral IPL, insula, IFG, middle and superior frontal gyri and thalamus (Fig. 5).

3.5. Behavioral decoding

In order to assess the functional roles of our seed regions, which represent the consistent evidence for PD-related intrinsic aberrations, we performed behavioral decoding using the BrainMap database. In detail, we tested which types of tasks were more likely to activate the

regions identified in the ALE analysis than by chance. We found significant associations ($p < .05$, corrected for multiple comparisons) of the posterior part of right IPL with perception (vision) and for the posterior part of left IPL with cognition, reasoning, explicit memory; the supramarginal gyrus showed significant association with perception (somesthesis), action and executive functions.

4. Discussion

Rs-fMRI has been widely applied in order to understand the functional architecture of the human brain by means of spontaneous neural activity while being at rest (Cole, Smith, & Beckmann, 2010). Unlike task-based fMRI it is relatively uninfluenced by compliance or task performance and thus has become increasingly popular to investigate clinical populations including PD. The currently available rs-fMRI imaging studies, however, often point to diverse and conflicting findings. In this study, we applied the ALE meta-analysis method to gain a better understanding of core features of intrinsic alteration in patients with PD across the literature. We integrated findings from 28 rs-fMRI studies and found convergent aberrations in PD patients predominantly in the IPL. That is, rather than, e.g., the striatum, the posterior IPL, a relatively neglected area in the PD neurocircuitry fingerprint, showed the most consistent disturbances in resting-state fMRI (Fig. 2). In particular, these findings were mainly driven by (i) increased functional parameters in PD patients deprived of their dopamine replacement therapy (OFF-state) in the left and right inferior parietal lobe as well as the right supramarginal gyrus, and (ii) decreased functional parameters in PD patients on dopamine replacement therapy (ON-state) in the right inferior parietal lobe. These findings highlighted the role of bilateral IPL and the supramarginal gyrus as the important nodes in PD and further suggested the intrinsic dysfunctional patterns of these regions as an early imaging biomarker of PD.

We then used the bilateral IPL and right supramarginal gyrus regions identified by the meta-analysis, as seed regions for MACM- and resting-state FC analysis in order to identify the networks related to these. Conjunction analyses between MACM and resting-state FC highlighted coupling between seeds and several areas not only in the IPL but in particular also in the middle and superior frontal gyri, posterior-medial frontal cortex, mid-cingulate cortex, orbitofrontal cortex, precentral, precuneus, PCC, insula, hippocampus and thalamus (Fig. 5). Behavioral characterization of the seeds using the BrainMap database suggested associated dysfunction of perception and executive functions.

4.1. The role of the parietal cortex in PD

Our ALE meta-analysis indicated that PD patients display altered intrinsic functional patterns, converging in bilateral IPL compared to healthy controls. Numerous human and animal studies have identified the parietal lobe as an “association cortex” implicated in a variety of functions encompassing not only higher motor control but among others also attentional processes, spatial representation, (eye) movements and working memory (for review see: Culham & Kanwisher, 2001). The heterogeneous nature of inferior parietal lobe functions is further demonstrated by patients suffering from damage in this region: They experience a range of impairments including attentional deficits such as spatial neglect

(Karnath & Rorden, 2012), autobiographical memory impairments (Berryhill, Phuong, Picasso, Cabeza, & Olson, 2007), contractual apraxia as well as visual mislocalization and visual disorientation (Andersen, 2011).

The IPL has been thought to operate as a sensorimotor interface important for guidance of movement via sensory feedback (Mattingley, Husain, Rorden, Kennard, & Driver, 1998). The integration of sensory feedback, particularly visual and proprioceptive input (Sober & Sabes, 2005), into planning and control of movements is essential in order to ensure the correct execution of a motor program (Abbruzzese & Berardelli, 2003). It has been suggested that the basal ganglia are responsible for gating sensory inputs from somatosensory cortices towards motor areas and that this gating function plays an important role for appropriate motor execution (Kaji, Urushihara, Murase, Shimazu, & Goto, 2005). In PD patients however, basal ganglia function is deprived, which in turn may lead to alterations in the sensorimotor system (Stoessl, Martin, McKeown, & Sossi, 2011). Although not a very prominent feature of PD per se, somatosensory abnormalities in patients have been observed in experimental settings [for a review see (Machado et al., 2010)]. In comparison with healthy controls, PD patients perform worse on tests of proprioception, e.g., during two-point discrimination (Schneider, Diamond, & Markham, 1987). Moreover, they show impairments in joint-position sense (Zia, Cody, & O'Boyle, 2002) and have difficulties to perform accurate movements when deprived of visual input of the moving limb (Klockgether & Dichgans, 1994) suggesting the notion that PD patients rely more on visual (as supposed to somatosensory) feedback while moving. Another ALE meta-analysis aimed to determine a common neural substrate for motor control deficits in PD (Herz et al., 2014) supports this idea. This work incorporated studies in which PD patients were asked to execute *externally* triggered movements during task fMRI or H_2O-PET. The results also indicated increased activation of the parietal lobe in PD patients in the OFF-state. Based on this finding, it was suggested that PD patients rely more on external cues during executing movements which may lead to increased activation of the IPL implying a compensatory role of this area during the production of motor output (Herz et al., 2014). Strikingly, even in an at-risk group for PD, namely asymptomatic individuals holding a mutation in the Parkin gene, sensorimotor integration impairments were observed underlining the early onset of possible IPL alterations in PD (Baumer et al., 2007). Thus, one might argue that increasing intrinsic activity in areas important for sensorimotor integration such as the IPL might be a strategy in order to compensate for disturbed processing of somatosensory input via the basal ganglia towards motor cortices.

In support of this view, it has recently been suggested that lack of dopamine in PD might lead to abnormal synchronization of oscillatory neural activity in the basal ganglia resulting in less efficient information processing (Brittain & Brown, 2014). PD patients deprived of their dopaminergic medication might therefore experience a processing deficit in highly dopamine-dependent regions. This might be overcome by increased activation or connectivity in other, less affected regions (Gorges et al., 2013; Sharman et al., 2013). Indeed, the observed intrinsic functional imbalance of the IPL seems evident in early states of the disease. Strikingly, a study on leucine-rich repeat kinase 2 (LRRK2) mutation carriers, a population with an elevated risk of developing PD, demonstrated that FC between the IPL and the putamen was aberrant from healthy controls (Helmich et al., 2015). Whereas healthy

individuals display a strong FC between the IPL and the dorsoposterior part of the putamen (as supposed to the ventroanterior section), this relationship was reversed in presymptomatic mutation carriers. Since the posterior part of the putamen suffers a greater dopaminergic lack, this suggests that the connectivity shift from posterior to anterior is a compensatory process in order to counter a possible processing deficit. Interestingly, the strength of this shift increased with age in the mutation carriers but not in the noncarriers, pointing to a further progression of the compensatory mechanism (Helmich et al., 2015). The same connectivity shift could be observed in PD patients, where it was stronger on the less affected side, again suggesting a compensatory mechanism (Helmich et al., 2010). These findings imply, that after an initial break down of efficient processing in the basal ganglia due to a lack of dopamine, the deficit is countered by increased connectivity in other brain regions. One might speculate that the IPL hyperconnectivity will continue to increase while transitioning from a pre-symptomatic stage to manifest PD (Helmich et al., 2010, 2015). In manifest PD, the compensatory mechanism will work best where dopamine levels are still high until the system is worn out and will start to break down in later disease stages (Helmich et al., 2010).

In addition, a study in parkinsonian primates has shown that dopamine depletion may lead to an increasing functional overlap and cross-talk of previously segregated cortico-striatal loops (Bergman et al., 1998). This loss of segregation might lead to attentional problems and impaired action selection when more than one task has to be performed. In support of this it was shown that PD patients seem impaired while performing dual-task paradigms comprising a motor and a cognitive challenge (Vervoort et al., 2016). In this study, the performance of a simple gait task was significantly decreased in patients when an auditory version of the stroop-task had to be completed at the same time. Better performance, however, was positively correlated with increased FC between the IPL and premotor as well as motor area M1. In contrast, FC during rest was decreased between the IPL and two sides of great dopaminergic deficit in PD, namely the caudate nucleus and SNc. A similar connectivity shift (i.e., increased FC) from strongly dopamine-dependent to other regions has also been observed when patients engaged in a cognitively demanding working memory task (Muller-Oehring et al., 2014). These finding again highlight its compensatory nature. In accordance, our analysis revealed not only increased intrinsic function in OFF-state patients, but also decreased intrinsic function after administration of dopaminergic medication. This finding is in line with a number of studies examining the effect of dopaminergic medication on connectivity patterns in PD. Aberrant FC in dopamine-deprived regions and connected areas has frequently been demonstrated and has been shown to be normalized with dopaminergic medication (Agosta et al., 2014; Kwak et al., 2010, 2012).

Recently, Wang and colleagues examined the functional organization of the left IPL during rest and during various tasks and demonstrated that the supramarginal gyrus is involved in sensorimotor processing, movement imagination and inhibitory control, audition perception and speech processing, and social cognition, while the angular gyrus is involved in episodic memory, semantic processing, and spatial cognition (Wang et al., 2017). This finding supports the important role of IPL in a number of functions, which are known to be affected in PD.

Taken together, it is conceivable that alteration of IPL intrinsic functional parameters as observed in our ALE meta-analysis might be an attempt to compensate for inefficient processing within the basal ganglia and that – together with a major dopamine deficit within the striatum– this might be one of the early factors contributing to typical symptoms in PD, specifically motor impairment.

4.2. Task-dependent and task-independent FC patterns

When using the bilateral IPL and the supramarginal gyrus as seeds for MACM and resting-state analyses, the observed task-dependent and task-independent FC patterns, respectively, partially overlapped with the brain's largest intrinsic network, the default mode network (DMN). The DMN encompasses brain areas including the ventral and lateral medial prefrontal cortex, lateral temporal cortex, hippocampal formation, posterior cingulate/retrospinal cortex and the posterior part of IPL (Buckner, Andrews-Hanna, & Schacter, 2008). Previously, it has been reported that the posterior part of IPL, which was the most consistent abnormal region based on our data is a part of the DMN (Davey, Pujol, & Harrison, 2016; Mars et al., 2012). The IPL is the most active in the resting brain or during visual fixation when no specific task is performed, but de-activation is observed when engaged in a cognitive task (Buckner et al., 2008; Greicius, Krasnow, Reiss, & Menon, 2003). A recent ALE meta-analysis examining the functions of the inferior parietal lobe identified four functionally dissociable clusters within this region (Bzdok, Reid, Laird, Fox, Eickhof, 2016). Interestingly, one cluster, which was found to be associated with the DMN, was located in PGa and PGp – the exact same regions to show aberrant FC in PD patients in our analysis. The DMN has been the focus of various tasked-based and rs-fMRI studies in the OFF- and ON-states in PD patients (Amboni et al., 2014; Baggio et al., 2014; Delaveau et al., 2010; Disbrow et al., 2014; Gorges et al., 2013; Rektorova, Krajcovicova, Marecek, & Mikl, 2012; Tessitore et al., 2012; van Eimeren, Monchi, Ballanger, & Strafella, 2009). It has been shown that lower activity in the SNc was associated with decreased DMN activity and that this was also associated with disease severity (Wu et al., 2012). Amboni et al. (2014) found that the disruption occurred even in absence of structural gray matter changes and that reduced FC within the fronto-parietal network was characteristic for PD patients with mild cognitive impairment. Moreover, others found that the reduced activation of the DMN during rest was not only a hallmark of PD per se, but also correlated with decreased processing speed and increased switch time during an executive task (Disbrow et al., 2014). However, the DMN in PD does not only seem to be disrupted during resting conditions. The typically observed "de-activation" occurring during a cognitively demanding task, seems to be aberrant in PD as well (Delaveau et al., 2010; van Eimeren et al., 2009). Delaveau and colleagues have shown that PD patients in the OFF-state are unable to successfully deactivate the DMN during a facial emotion recognition task. The activation or rather "non-deactivation " of the posterior DMN during task demands was thought to be a consequence of dopamine depletion within the putamen and thus was interpreted as being compensatory in order to keep cognitive performance high. However, when levodopa was administered the disrupted deactivation could be normalized (Delaveau et al., 2010). Similarly, higher resting-state FC has been interpreted as an inability to suppress the DMN in turns resulting in the inability to switch to task-related networks when a task is performed (Trujillo et al., 2015). Whereas the overall connectivity throughout the brain increases, connectivity within or

between regions, implicated in a certain task (e.g., during a working memory challenge), may decrease. This imbalance might thus lead to an overall decreased signal-to-noise ratio and consequently slightly worse cognitive performance (Trujillo et al., 2015). A recent neuroimaging meta-analysis based on 10 ReHo studies in PD (in the OFF-state) found a convergent increased ReHo in the DMN, mainly in bilateral IPL and mPFC. The authors suggested that this observed increased ReHo reflects a compensatory mechanism to retain patients' cognitive performance (Pan et al., 2017).

Our MACM and resting-state FC analyses also revealed that the supramarginal gyrus, a region showing convergent differences in the "PD-OFF > Controls" contrasts, had significant FC with several brain areas including the bilateral IPL, insula, IFG, middle and superior frontal gyri, thalamus, and midcingulate cortex. This finding might also be related to associated dysfunction in perception and executive functions in PD. Previous studies have shown dysfunction of preSMA (Eckert, Peschel, Heinze, & Rotte, 2006; MacDonald & Halliday, 2002), mid-cingulate cortex (Hoffstaedter et al., 2014), prefrontal cortex (Srovnalova, Marecek, & Rektorova, 2011; Tahmasian, Rochhausen, et al., 2015), insula (Christopher, Koshimori, Lang, Criaud, & Strafella, 2014), and thalamus (Halliday, 2009) in PD, which are responsible for motor and non-motor symptoms of PD.

In general, our connectivity analyses demonstrated that the observed convergent seeds are part of the joint networks, which is an important finding to understand pathophysiology of PD. In particular, the posterior part of IPL was connected mainly with the DMN subregions. Disruption of the DMN been shown to be related to non-motor symptoms and cognitive decline in PD. Moreover, the supramarginal gyrus was connected to several regions associated with perception and executive functions, which are also disrupted in PD. In addition, behavioral characterization of these seed regions using the BrainMap database further highlighted associated dysfunction of perception and executive functions in PD.

4.3. Potential strength and limitations

A major advantage of our ALE meta-analysis approach is the integration of a great number of subjects to establish consensus on the locations of functional or structural disruptions in neuropsychiatric disorders across previously published studies (Eickhoff & Bzdok, 2013; Eickhoff et al., 2012; Tahmasian et al., 2016). Multiple comparisons correction of neuroimaging findings is a critical step to ensure statistical rigor of such studies. Recently, it has been revealed that the routine statistical inferences in cluster levels of some neuroimaging studies might permeate the results and distend the false-positive findings (Eklund, Nichols, & Knutsson, 2016). In this study, we performed multiple-comparison correction using the cluster-level FWE correction, which is recently suggested to be used for ALE analyses in preference to false discovery rate (FDR) to provide maximum statistical rigor (Eickhoff et al., 2017).

The 63 experiments included in our meta-analysis are different regarding to design, methodology, age and gender of population. In addition, we did not focus on a certain subgroup of PD patients but included patients ranging from a de-novo state to manifest PD with high UPDRS-scores, tremor-and gait-dominant patients as well as patients with and without cognitive impairment. This meta-analysis approach gives us the unique opportunity

to focus on the commonality between all those patients, rather than the differences between subgroups. However, one can apply ALE analysis in particular subgroups of PD in future, when there are enough available rs-fMRI data to do so. Of note, one should be aware of the fact that our CBMA approach uses precise coordinates (rather than general regional labels) as its input and these foci are limited indicators of the location of a significant anatomical difference (Wager, Lindquist, Nichols, Kober, & Van Snellenberg, 2009). In this method, overlapping difference clusters are usually found by averaging across various peak coordinates, increasing the risk that with two or more relatively nearby peak foci, ALE will find an average significant cluster somewhere between these foci in a brain region that was actually not reported in the source studies (Eickhoff & Bzdok, 2013; Wager et al., 2009). In addition, it has been suggested that image-based meta-analysis is preferred over CBMA because CBMA provide less information from each study (Salimi-Khorshidi, Smith, Keltner, Wager, & Nichols, 2009). However, the original data is often difficult to obtain from individual studies compared to the reported peak coordinates. Therefore, CBMA is still the standard ALE approach to identify common regional abnormalities (Eickhoff & Bzdok, 2013).

It has to be mentioned that although the individual studies mostly matched their groups for age or gender, we did not control for such covariates across included studies due to current methodological ALE limitations and low number of included studies. Of note is that although a previous meta-analysis in PD based on motor task fMRI studies found increased activation of parietal cortex in PD patients in the OFF medication compared to healthy controls, which is similar to our results, we did not identify any effect within the basal ganglia, the main side of dopamine depletion in PD (Herz et al., 2014). Moreover, Herz and colleagues found significant convergence of activation between PD-ON and PD-OFF conditions in the right middle frontal gyrus and right putamen among 10 task fMRI experiments (Herz et al., 2014). However, although we previously suggested that dopamine replacement therapy normalize the functional abnormalities in PD (Tahmasian, Bettray, et al., 2015), there were not sufficient rs-fMRI studies to provide significant results in the “PD-OFF” versus “PD-ON” contrasts here.

In a recent PD meta-analysis, Pan and colleagues found a convergent lower ReHo in the right putamen and right precentral gyrus using an uncorrected statistical threshold (Pan et al., 2017). In our study, however, we did not observe any significant consistent changes in basal ganglia using the cluster-level FWE correction. This might be due to the fact that rs-fMRI studies in PD used heterogeneous preprocessing and analysis approaches (Tahmasian, Bettray, et al., 2015). More specifically, most of the included studies applied graph analyses and ICA methods, focusing on the DMN, as well as voxel-wise regional approaches (ALFF, ReHo). In the present meta-analysis, we also excluded all seed-based FC studies, the majority of which seeded the basal ganglia, to avoid prior selection bias. Furthermore, our findings might be dependent upon the clinical heterogeneity of PD patients across studies including hallucination, depression, and cognitive impairment. One should note that ALFF and ReHo are measuring the BOLD signal in a local manner, whereas FC is usually described as inter-regional covariance. Thus, our findings demonstrate both local and inter-regional functional alterations in PD.

5. Conclusion

Using the ALE approach, we here demonstrated that across the entire available rs-fMRI literature, PD patients display abnormal intrinsic functional patterns converging in the bilateral posterior IPL extending towards the TPJ. Notably, whereas intrinsic functional patterns in OFF-state patients were increased in these regions, it was decreased in medicated patients. This pattern could indicate a compensatory process countering inefficient processing within the basal ganglia due to dopamine depletion. This view is in line with previous reports showing alterations within the IPL in high-risk populations even before the onset of overt symptoms. MACM and resting-state FC analyses showed that the posterior part of IPL and supramarignal gyrus are strongly connected with a wide range of brain structures, partially resembling the DMN. One might argue that altered intrinsic functional patterns within the IPL may lead to further disruption in functionally connected areas. This idea is supported by a number of studies in PD patients demonstrating DMN disruptions during rest and the inefficient deactivation of this network during task performance early in the course of the disease even in absence of structural gray matter changes. In summary, we revealed that PD patients display abnormal intrinsic functional patterns in the posterior part of IPL in the ON- and OFF-state and that this region is connected to other areas that have been shown to be disrupted in early stage patients and even high-risk groups. Thus, it might be feasible to use intrinsic functional patterns of the IPL as an early imaging biomarker of PD even before the onset of overt motor symptoms.

Supplementary Material

Refer to Web version on PubMed Central for supplementary material.

Acknowledgements

This study was supported by Deutsche For-schungsgemeinschaft (DFG), KFO 219, TP10, EG 350/1-1, EI 816/4-1, LA 3071/3-1; EI 816/6-1, the National Institute of Mental Health (R01-MH074457), the Helmholtz Portfolio Theme “Supercomputing and Modeling for the Human Brain” and the European Union Seventh Framework Programme (FP7/2007-2013) under grant agreement no. 604102.

REFERENCES

Abbruzzese G, & Berardelli A (2003). Sensorimotor integration in movement disorders. Movement Disorders, 18(3), 231–240. 10.1002/mds.10327. [PubMed: 12621626]

Agosta F, Caso F, Stankovic I, Inuggi A, Petrovic I, Svetel M, et al. (2014). Cortico-striatal-thalamic network functional connectivity in hemiparkinsonism. Neurobiology of Aging, 35(11), 2592–2602. 10.1016/j.neurobiolaging.2014.05.032. [PubMed: 25004890]

Amboni M, Tessitore A, Esposito F, Santangelo G, Picillo M, Vitale C, et al. (2014). Resting-state functional connectivity associated with mild cognitive impairment in Parkinson’s disease. Journal of Neurology, 262(2), 425–434. 10.1007/s00415-014-7591-5. [PubMed: 25428532]

Amft M, Bzdok D, Laird AR, Fox PT, Schilbach L, & Eickhoff SB (2015). Definition and characterization of an extended social-affective default network. Brain Structure & Function, 220(2), 1031–1049. 10.1007/s00429-013-0698-0. [PubMed: 24399179]

Amunts K, Schleicher A, Burgel U, Mohlberg H, Uylings HB, & Zilles K (1999). Broca’s region revisited: Cytoarchitecture and intersubject variability. Journal of Comparative Neurology, 412(2), 319–341.

Andersen RA (2011). Inferior parietal lobule function in spatial perception and visuomotor integration. Comprehensive Physiology, 483–518. http://onlinelibrary.wiley.com/doi/10.1002/cphy.cp010512/abstract.

Baggio HC, Sala-Llonch R, Segura B, Marti MJ, Valldeoriola F, Compta Y, et al. (2014). Functional brain networks and cognitive deficits in Parkinson's disease. Human Brain Mapping, 35(9), 4620–4634. 10.1002/hbm.22499. [PubMed: 24639411]

Baumer T, Pramstaller PP, Siebner HR, Schippling S, Hagenah J, Peller M, et al. (2007). Sensorimotor integration is abnormal in asymptomatic Parkin mutation carriers: A TMS study. Neurology, 69(21), 1976–1981. 10.1212/01.wnl.0000278109.76607.0a. [PubMed: 18025391]

Behrens TEJ, Johansen-Berg H, Woolrich MW, Smith SM, Wheeler-Kingshott CAM, Boulby PA, et al. (2003). Noninvasive mapping of connections between human thalamus and cortex using diffusion imaging. Nature Neuroscience, 6(7), 750–757. 10.1038/nn1075. [PubMed: 12808459]

Bergman H, Feingold A, Nini A, Raz A, Slovin H, Abeles M, et al. (1998). Physiological aspects of information processing in the basal ganglia of normal and parkinsonian primates. Trends in Neurosciences, 21(1), 32–38. [PubMed: 9464684]

Berryhill ME, Phuong L, Picasso L, Cabeza R, & Olson IR (2007). Parietal lobe and episodic memory: Bilateral damage causes impaired free recall of autobiographical memory. The Journal of Neuroscience, 27(52), 14415–14423. 10.1523/JNEUROSCI.4163-07.2007. [PubMed: 18160649]

Biswal BB (2012). Resting state fMRI: A personal history. NeuroImage, 62(2), 938–944. 10.1016/j.neuroimage.2012.01.090. [PubMed: 22326802]

Borroni B, Premi E, Formenti A, Turrone R, Alberici A, Cottini E, et al. (2015). Structural and functional imaging study in dementia with Lewy bodies and Parkinson's disease dementia. Parkinsonism & Related Disorders, 21(9), 1049–1055. 10.1016/j.parkreldis.2015.06.013. [PubMed: 26109553]

Braak H, Del Tredici K, Rub U, de Vos RA, Jansen Steur EN, & Braak E (2003). Staging of brain pathology related to sporadic Parkinson's disease. Neurobiology of Aging, 24(2), 197–211. [PubMed: 12498954]

Braak H, Ghebremedhin E, Rub U, Bratzke H, & Del Tredici K (2004). Stages in the development of Parkinson's disease-related pathology. Cell and Tissue Research, 318(1), 121–134. 10.1007/s00441-004-0956-9. [PubMed: 15338272]

Brittain JS, & Brown P (2014). Oscillations and the basal ganglia: Motor control and beyond. NeuroImage, 85(Pt 2), 637–647. 10.1016/j.neuroimage.2013.05.084. [PubMed: 23711535]

Buckner RL, Andrews-Hanna JR, & Schacter DL (2008). The brain's default network: Anatomy, function, and relevance to disease. Annals of the New York Academy of Sciences, 1124, 1–38. 10.1196/annals.1440.011. [PubMed: 18400922]

Bzdok D, Heeger A, Langner R, Laird AR, Fox PT, Palomero-Gallagher N, et al. (2015). Subspecialization in the human posterior medial cortex. NeuroImage, 106, 55–71. 10.1016/j.neuroimage.2014.11.009. [PubMed: 25462801]

Bzdok D, Langner R, Schilbach L, Engemann DA, Laird AR, Fox PT, et al. (2013). Segregation of the human medial prefrontal cortex in social cognition. Frontiers in Human Neuroscience, 7, 232. 10.3389/Fnhum.2013.00232. [PubMed: 23755001]

Bzdok D, Langner R, Schilbach L, Jakobs O, Roski C, Caspers S, et al. (2013). Characterization of the temporoparietal junction by combining data-driven parcellation, complementary connectivity analyses, and functional decoding. NeuroImage, 81, 381–392. 10.1016/j.neuroimage.2013.05.046. [PubMed: 23689016]

Bzdok DHG, Reid A, Laird AR, Fox PT, & Eickhof SB (2016). Left inferior parietal lobe engagement in social cognition and language. Neuroscience and Biobehavioral Reviews.

Caspers S, Eickhoff SB, Geyer S, Scheperjans F, Mohlberg H, Zilles K, et al. (2008). The human inferior parietal lobule in stereotaxic space. Brain Structure & Function, 212(6), 481–495. 10.1007/s00429-008-0195-z. [PubMed: 18651173]

Caspers S, Geyer S, Schleicher A, Mohlberg H, Amunts K, & Zilles K (2006). The human inferior parietal cortex: Cytoarchitectonic parcellation and interindividual variability. NeuroImage, 33(2), 430–448. 10.1016/j.neuroimage.2006.06.054. [PubMed: 16949304]

Caspers J, Zilles K, Amunts K, Laird AR, Fox PT, & Eickhoff SB (2014). Functional characterization and differential coactivation patterns of two cytoarchitectonic visual areas on the human posterior fusiform gyrus. Human Brain Mapping, 35(6), 2754–2767. 10.1002/hbm.22364. [PubMed: 24038902]

Chaudhuri KR, Healy DG, Schapira AH, & National Institute for Clinical, E. (2006). Non-motor symptoms of Parkinson's disease: Diagnosis and management. Lancet Neurology, 5(3), 235–245. 10.1016/S1474-4422(06)70373-8. [PubMed: 16488379]

Chen HM, Wang ZJ, Fang JP, Gao LY, Ma LY, Wu T, et al. (2015). Different patterns of spontaneous brain activity between tremor-dominant and postural instability/gait difficulty subtypes of Parkinson's disease: A resting-state fMRI study. CNS Neuroscience & Therapeutics, 21(10), 855–866. 10.1111/cns.12464. [PubMed: 26387576]

Choe IH, Yeo S, Chung KC, Kim SH, & Lim S (2013). Decreased and increased cerebral regional homogeneity in early Parkinson's disease. Brain Research, 1527, 230–237. 10.1016/j.brainres.2013.06.027. [PubMed: 23816374]

Christopher L, Koshimori Y, Lang AE, Criaud M, & Strafella AP (2014). Uncovering the role of the insula in non-motor symptoms of Parkinson's disease. Brain, 137(Pt 8), 2143–2154. 10.1093/brain/awu084. [PubMed: 24736308]

Clos M, Rottschy C, Laird AR, Fox PT, & Eickhoff SB (2014). Comparison of structural covariance with functional connectivity approaches exemplified by an investigation of the left anterior insula. NeuroImage, 99, 269–280. 10.1016/j.neuroimage.2014.05.030. [PubMed: 24844743]

Cole DM, Smith SM, & Beckmann CF (2010). Advances and pitfalls in the analysis and interpretation of resting-state FMRI data. Frontiers in Systems Neuroscience, 4, 8. 10.3389/fnsys.2010.00008. [PubMed: 20407579]

Costafreda SG, Fu CH, Lee L, Everitt B, Brammer MJ, & David AS (2006). A systematic review and quantitative appraisal of fMRI studies of verbal fluency: Role of the left inferior frontal gyrus. Human Brain Mapping, 27(10), 799–810. 10.1002/hbm.20221. [PubMed: 16511886]

Culham JC, & Kanwisher NG (2001). Neuroimaging of cognitive functions in human parietal cortex. Current Opinion in Neurobiology, 11(2), 157–163. [PubMed: 11301234]

Davey CG, Pujol J, & Harrison BJ (2016). Mapping the self in the brain's default mode network. NeuroImage, 132, 390–397. 10.1016/j.neuroimage.2016.02.022. [PubMed: 26892855]

Delaveau P, Salgado-Pineda P, Fossati P, Witjas T, Azulay JP, & Blin O (2010). Dopaminergic modulation of the default mode network in Parkinson's disease. European Neuropsychopharmacology, 20(11), 784–792. 10.1016/j.euroneuro.2010.07.001. [PubMed: 20674286]

Del Tredici K, Rub U, De Vos RA, Bohl JR, & Braak H (2002). Where does parkinson disease pathology begin in the brain? Journal of Neuropathology and Experimental Neurology, 61(5), 413–426. [PubMed: 12030260]

Di Martino A, Scheres A, Margulies DS, Kelly AMC, Uddin LQ, Shehzad Z, et al. (2008). Functional connectivity of human striatum: A resting state fMRI study. Cerebral Cortex, 18(12), 2735–2747. 10.1093/cercor/bhn041. [PubMed: 18400794]

Disbrow EA, Carmichael O, He J, Lanni KE, Dressler EM, Zhang L, et al. (2014). Resting state functional connectivity is associated with cognitive dysfunction in non-demented people with Parkinson's disease. Journal of Parkinson's Disease, 4(3), 453–465. 10.3233/JPD-130341.

Evans AC, Collins DL, Mills SR, Brown ED, Kelly RL, & Peters TM (1993). 3D statistical neuroanatomical models from 305 MRI volumes. In Nuclear Science Symposium and Medical Imaging Conference, IEEE Conference Record (pp. 1813–1817). 10.1109/NSSMIC.1993.373602.

Eckert T, Peschel T, Heinze HJ, & Rotte M (2006). Increased pre-SMA activation in early PD patients during simple self-initiated hand movements. Journal of Neurology, 253(2), 199–207. 10.1007/s00415-005-0956-z. [PubMed: 16222427]

Eckert T, Tang C, & Eidelberg D (2007). Assessment of the progression of Parkinson's disease: A metabolic network approach. Lancet Neurology, 6(10), 926–932. 10.1016/S1474-4422(07)70245-4. [PubMed: 17884682]

Eickhoff S, & Bzdok D (2013). Meta-analyses in basic and clinical Neuroscience: State of the art and perspective. In Ulmer S, & Jansen O (Eds.), fMRI (pp. 77–87). Springer Berlin Heidelberg.

Eickhoff SB, Bzdok D, Laird AR, Kurth F, & Fox PT (2012). Activation likelihood estimation meta-analysis revisited. NeuroImage, 59(3), 2349–2361. 10.1016/j.neuroimage.2011.09.017. [PubMed: 21963913]

Eickhoff SB, Bzdok D, Laird AR, Roski C, Caspers S, Zilles K, et al. (2011). Co-activation patterns distinguish cortical modules, their connectivity and functional differentiation. NeuroImage, 57(3), 938–949. 10.1016/j.neuroimage.2011.05.021. [PubMed: 21609770]

Eickhoff SB, Laird AR, Fox PM, Lancaster JL, & Fox PT (2017). Implementation errors in the GingerALE Software: Description and recommendations. Human Brain Mapping, 38(1), 7–11. 10.1002/hbm.23342. [PubMed: 27511454]

Eickhoff SB, Laird AR, Grefkes C, Wang LE, Zilles K, & Fox PT (2009). Coordinate-based activation likelihood estimation meta-analysis of neuroimaging data: A random-effects approach based on empirical estimates of spatial uncertainty. Human Brain Mapping, 30(9), 2907–2926. 10.1002/hbm.20718. [PubMed: 19172646]

Eickhoff SB, Lotze M, Wietek B, Amunts K, Enck P, & Zilles K (2006). Segregation of visceral and somatosensory afferents: An fMRI and cytoarchitectonic mapping study. NeuroImage, 31(3), 1004–1014. 10.1016/j.neuroimage.2006.01.023. [PubMed: 16529950]

Eickhoff SB, Stephan KE, Mohlberg H, Grefkes C, Fink GR, Amunts K, et al. (2005). A new SPM toolbox for combining probabilistic cytoarchitectonic maps and functional imaging data. NeuroImage, 25(4), 1325–1335. 10.1016/j.neuroimage.2004.12.034. [PubMed: 15850749]

van Eimeren T, Monchi O, Ballanger B, & Strafella AP (2009). Dysfunction of the default mode network in Parkinson disease: A functional magnetic resonance imaging study. Archives of Neurology, 66(7), 877–883. 10.1001/archneurol.2009.97. [PubMed: 19597090]

Eklund A, Nichols TE, & Knutsson H (2016). Cluster failure: Why fMRI inferences for spatial extent have inflated false-positive rates. Proceedings of the National Academy of Sciences of the United States of America, 113(28), 7900–7905. 10.1073/pnas.1602413113. [PubMed: 27357684]

Esposito F, Tessitore A, Giordano A, De Micco R, Paccone A, Conforti R, et al. (2013). Rhythm-specific modulation of the sensorimotor network in drug-naive patients with Parkinson's disease by levodopa. Brain, 136(Pt 3), 710–725. 10.1093/brain/awt007. [PubMed: 23423673]

Fox PT, Laird AR, Fox SP, Fox PM, Uecker AM, Crank M, et al. (2005). BrainMap taxonomy of experimental design: Description and evaluation. Human Brain Mapping, 25(1), 185–198. 10.1002/hbm.20141. [PubMed: 15846810]

Fox MD, Snyder AZ, Vincent JL, Corbetta M, Van Essen DC, & Raichle ME (2005). The human brain is intrinsically organized into dynamic, anticorrelated functional networks. Proceedings of the National Academy of Sciences of the United States of America, 102(27), 9673–9678. 10.1073/pnas.0504136102. [PubMed: 15976020]

Goodkind M, Eickhoff SB, Oathes DJ, Jiang Y, Chang A, Jones-Hagata LB, et al. (2015). Identification of a common neurobiological substrate for mental illness. JAMA Psychiatry, 72(4), 305–315. 10.1001/jamapsychiatry.2014.2206. [PubMed: 25651064]

Gorges M, Muller HP, Lule D, Consortium L, Pinkhardt EH, Ludolph AC, et al. (2015). To rise and to fall: Functional connectivity in cognitively normal and cognitively impaired patients with Parkinson's disease. Neurobiology of Aging, 36(4), 1727–1735. 10.1016/j.neurobiolaging.2014.12.026. [PubMed: 25623332]

Gorges M, Muller HP, Lule D, Ludolph AC, Pinkhardt EH, & Kassubek J (2013). Functional connectivity within the default mode network is associated with saccadic accuracy in Parkinson's disease: A resting-state FMRI and videooculographic study. Brain Connectivity, 3(3), 265–272. 10.1089/brain.2013.0146. [PubMed: 23627641]

Gottlich M, Munte TF, Heldmann M, Kasten M, Hagenah J, & Kramer UM (2013). Altered resting state brain networks in Parkinson's disease. PLoS One, 8(10), e77336. 10.1371/journal.pone.0077336. [PubMed: 24204812]

Greicius MD, Krasnow B, Reiss AL, & Menon V (2003). Functional connectivity in the resting brain: A network analysis of the default mode hypothesis. Proceedings of the National Academy of Sciences of the United States of America, 100(1), 253–258. 10.1073/pnas.0135058100. [PubMed: 12506194]

Halliday GM (2009). Thalamic changes in Parkinson's disease. Parkinsonism & Related Disorders, 15(Suppl. 3), S152–S155. 10.1016/S1353-8020(09)70804-1. [PubMed: 20082979]

Helmich RC, Derikx LC, Bakker M, Scheeringa R, Bloem BR, & Toni I (2010). Spatial remapping of corticostriatal connectivity in Parkinson's disease. Cerebral Cortex, 20(5), 1175–1186. 10.1093/cercor/bhp178. [PubMed: 19710357]

Helmich RC, Thaler A, van Nuenen BF, Gurevich T, Mirelman A, Marder KS, et al. (2015). Reorganization of corticostriatal circuits in healthy G2019S LRRK2 carriers. Neurology, 84(4), 399–406. 10.1212/WNL.0000000000001189. [PubMed: 25540317]

Herz DM, Eickhoff SB, Lokkegaard A, & Siebner HR (2014). Functional neuroimaging of motor control in Parkinson's disease: A meta-analysis. Human Brain Mapping, 35(7), 3227–3237. 10.1002/hbm.22397. [PubMed: 24123553]

Hoffstaedter F, Grefkes C, Caspers S, Roski C, Palomero-Gallagher N, Laird AR, et al. (2014). The role of anterior midcingulate cortex in cognitive motor control: Evidence from functional connectivity analyses. Human Brain Mapping, 35(6), 2741–2753. 10.1002/hbm.22363. [PubMed: 24115159]

Hou Y, Wu X, Hallett M, Chan P, & Wu T (2014). Frequency-dependent neural activity in Parkinson's disease. Human Brain Mapping, 35(12), 5815–5833. 10.1002/hbm.22587. [PubMed: 25045127]

Hu XF, Zhang JQ, Jiang XM, Zhou CY, Wei LQ, Yin XT, et al. (2015). Amplitude of low-frequency oscillations in Parkinson's disease: A 2-year longitudinal resting-state functional magnetic resonance imaging study. Chinese Medical Journal, 128(5), 593–601. 10.4103/0366-6999.151652. [PubMed: 25698189]

Jankovic J (2008). Parkinson's disease: Clinical features and diagnosis. Journal of Neurology Neurosurgery and Psychiatry, 79(4), 368–376. 10.1136/jnnp.2007.131045.

Kaji R, Urushihara R, Murase N, Shimazu H, & Goto S (2005). Abnormal sensory gating in basal ganglia disorders. Journal of Neurology, 252(Suppl. 4), IV13–IV16. 10.1007/s00415-005-4004-9. [PubMed: 16222432]

Karnath HO, & Rorden C (2012). The anatomy of spatial neglect. Neuropsychologia, 50(6), 1010–1017. 10.1016/j.neuropsychologia.2011.06.027. [PubMed: 21756924]

Khazaie H, Veronese M, Noori K, Emamian F, Zarei M, Ashkan K, et al. (2017 3 23). Functional reorganization in obstructive sleep apnoea and insomnia: A systematic review of the resting-state fMRI. Neuroscience & Biobehavioral Reviews, 77, 219–231. 10.1016/j.neubiorev.2017.03.013. [PubMed: 28344075]

Klockgether T, & Dichgans J (1994). Visual control of arm movement in Parkinson's disease. Movement Disorders, 9(1), 48–56. 10.1002/mds.870090108. [PubMed: 8139605]

Klupp E, Grimmer T, Tahmasian M, Sorg C, Yakushev I, Yousefi BH, et al. (2015). Prefrontal hypometabolism in Alzheimer disease is related to longitudinal amyloid accumulation in remote brain regions. Journal of Nuclear Medicine, 56(3), 399–404. 10.2967/jnumed.114.149302. [PubMed: 25678488]

Krall SC, Rottschy C, Oberwelland E, Bzdok D, Fox PT, Eickhoff SB, et al. (2015). The role of the right temporoparietal junction in attention and social interaction as revealed by ALE meta-analysis. Brain Structure & Function, 220(2), 587–604. 10.1007/s00429-014-0803-z. [PubMed: 24915964]

Kurth F, Zilles K, Fox PT, Laird AR, & Eickhoff SB (2010). A link between the systems: Functional differentiation and integration within the human insula revealed by meta-analysis. Brain Structure & Function, 214(5–6), 519–534. 10.1007/s00429-010-0255-z. [PubMed: 20512376]

Kwak Y, Peltier S, Bohnen NI, Muller ML, Dayalu P, & Seidler RD (2010). Altered resting state cortico-striatal connectivity in mild to moderate stage Parkinson's disease. Frontiers in Systems Neuroscience, 4, 143. 10.3389/fnsys.2010.00143. [PubMed: 21206528]

Kwak Y, Peltier SJ, Bohnen NI, Muller ML, Dayalu P, & Seidler RD (2012). L-DOPA changes spontaneous low-frequency BOLD signal oscillations in Parkinson's disease: A resting state fMRI study. Frontiers in Systems Neuroscience, 6, 52. 10.3389/fnsys.2012.00052. [PubMed: 22783172]

Laird AR, Eickhoff SB, Fox PM, Uecker AM, Ray KL, Saenz JJ Jr., et al. (2011). The BrainMap strategy for standardization, sharing, and meta-analysis of neuroimaging data. BMC Research Notes, 4, 349. 10.1186/1756-0500-4-349. [PubMed: 21906305]

Laird AR, Eickhoff SB, Kurth F, Fox PM, Uecker AM, Turner JA, et al. (2009). ALE meta-analysis workflows via the brainmap database: Progress towards a probabilistic functional brain atlas. Frontiers in Neuroinformatics, 3, 23. 10.3389/neuro.11.023.2009. [PubMed: 19636392]

Laird AR, Eickhoff SB, Li K, Robin DA, Glahn DC, & Fox PT (2009). Investigating the functional heterogeneity of the default mode network using coordinate-based meta-analytic modeling. Journal of Neuroscience, 29(46), 14496–14505. 10.1523/JNEUROSCI.4004-09.2009. [PubMed: 19923283]

Laird AR, Eickhoff SB, Rottschy C, Bzdok D, Ray KL, & Fox PT (2013). Networks of task co-activations. NeuroImage, 80, 505–514. 10.1016/j.neuroimage.2013.04.073. [PubMed: 23631994]

Lancaster JL, Tordesillas-Gutierrez D, Martinez M, Salinas F, Evans A, Zilles K, et al. (2007). Bias between MNI and talairach coordinates analyzed using the ICBM-152 brain template. Human Brain Mapping, 28(11), 1194–1205. 10.1002/hbm.20345. [PubMed: 17266101]

de Lau LML, & Breteler MMB (2006). Epidemiology of Parkinson's disease. Lancet Neurology, 5(6), 525–535. 10.1016/S1474-4422(06)70471-9. [PubMed: 16713924]

Lee MH, Smyser CD, & Shimony JS (2013). Resting-state fMRI: A review of methods and clinical applications. AJNR. American Journal of Neuroradiology, 34(10), 1866–1872. 10.3174/ajnr.A3263. [PubMed: 22936095]

Luo C, Chen Q, Song W, Chen K, Guo X, Yang J, et al. (2014). Resting-state fMRI study on drug-naive patients with Parkinson's disease and with depression. Journal of Neurology Neurosurgery and Psychiatry, 85(6), 675–683. 10.1136/jnnp-2013-306237.

MacDonald V, & Halliday GM (2002). Selective loss of pyramidal neurons in the pre-supplementary motor cortex in Parkinson's disease. Movement Disorders, 17(6), 1166–1173. 10.1002/mds.10258. [PubMed: 12465053]

Machado S, Cunha M, Velasques B, Minc D, Teixeira S, Domingues CA, et al. (2010). Sensorimotor integration: Basic concepts, abnormalities related to movement disorders and sensorimotor training-induced cortical reorganization. Revista de Neurologia, 51(7), 427–436. [PubMed: 20859923]

Madhyastha TM, Askren MK, Zhang J, Leverenz JB, Montine TJ, & Grabowski TJ (2015). Group comparison of spatiotemporal dynamics of intrinsic networks in Parkinson's disease. Brain, 138(Pt 9), 2672–2686. 10.1093/brain/awv189. [PubMed: 26173859]

Mars RB, Neubert FX, Noonan MP, Sallet J, Toni I, & Rushworth MF (2012). On the relationship between the "default mode network" and the "social brain". Frontiers in Human Neuroscience, 6, 189. 10.3389/fnhum.2012.00189. [PubMed: 22737119]

Mattingley JB, Husain M, Rorden C, Kennard C, & Driver J (1998). Motor role of human inferior parietal lobe revealed in unilateral neglect patients. Nature, 392(6672), 179–182. 10.1038/32413. [PubMed: 9515962]

Meng C, Brandl F, Tahmasian M, Shao J, Manoliu A, Scherr M, et al. (2014). Aberrant topology of striatum's connectivity is associated with the number of episodes in depression. Brain, 137(Pt 2), 598–609. 10.1093/brain/awt290. [PubMed: 24163276]

Moher D, Liberati A, Tetzlaff J, Altman DG, & Group P (2009). Preferred reporting items for systematic reviews and meta-analyses: The PRISMA statement. PLos Medicine, 6(7), e1000097. 10.1371/journal.pmed.1000097. [PubMed: 19621072]

Muller VI, Cieslik EC, Laird AR, Fox PT, & Eickhoff SB (2013). Dysregulated left inferior parietal activity in schizophrenia and depression: Functional connectivity and characterization. Frontiers in Human Neuroscience, 7, 268. 10.3389/fnhum.2013.00268. [PubMed: 23781190]

Muller VI, Cieslik EC, Serbanescu I, Laird AR, Fox PT, & Eickhoff SB (2016). Altered brain activity in unipolar depression revisited: Meta-analyses of neuroimaging studies. JAMA Psychiatry. 10.1001/jamapsychiatry.2016.2783.

Muller-Oehring EM, Sullivan EV, Pfefferbaum A, Huang NC, Poston KL, Bronte-Stewart HM, et al. (2014). Task-rest modulation of basal ganglia connectivity in mild to moderate Parkinson's disease. Brain Imaging and Behavior 10.1007/s11682-014-9317-9.

Nachev P, Kennard C, & Husain M (2008). Functional role of the supplementary and pre-supplementary motor areas. Nature Reviews Neuroscience, 9(11), 856–869. 10.1038/nrn2478. [PubMed: 18843271]

Nooner KB, Colcombe SJ, Tobe RH, Mennes M, Benedict MM, Moreno AL, et al. (2012). The NKI-Rockland sample: A model for accelerating the pace of discovery science in psychiatry. Frontiers in Neuroscience, 6, 152. 10.3389/fnins.2012.00152. [PubMed: 23087608]

Onu M, Badea L, Roceanu A, Tivarus M, & Bajenaru O (2015). Increased connectivity between sensorimotor and attentional areas in Parkinson's disease. Neuroradiology, 57(9), 957–968. 10.1007/s00234-015-1556-y. [PubMed: 26174425]

Pan P, Zhan H, Xia M, Zhang Y, Guan D, & Xu Y (2017). Aberrant regional homogeneity in Parkinson's disease: A voxel-wise meta-analysis of resting-state functional magnetic resonance imaging studies. Neuroscience and Biobehavioral Reviews, 72, 223–231. 10.1016/j.neubiorev.2016.11.018. [PubMed: 27916710]

Pasquini LSM, Tahmasian M, Meng C, Myers NE, Ortner M, Mühlau M, et al. (2014). Link between hippocampus' raised local and eased global intrinsic connectivity in AD. Alzheimer and Dementia. 10.1016/j.jalz.2014.02.007.

Prodoehl J, Burciu RG, & Vaillancourt DE (2014). Resting state functional magnetic resonance imaging in Parkinson's disease. Current Neurology and Neuroscience Reports, 14(6), 448. 10.1007/s11910-014-0448-6. [PubMed: 24744021]

Rana AQ, Masroor MS, & Khan AS (2013). A review of methods used to study cognitive deficits in Parkinson's disease. Neurological Research, 35(1), 1–6. 10.1179/1743132812Y.0000000118. [PubMed: 23317792]

Rektorova I, Krajcovicova L, Marecek R, & Mikl M (2012). Default mode network and extrastriate visual resting state network in patients with Parkinson's disease dementia. Neurodegenerative Diseases, 10(1–4), 232–237. 10.1159/000334765. [PubMed: 22269223]

Riedl V, Bienkowska K, Strobel C, Tahmasian M, Grimmer T, Forster S, et al. (2014). Local activity determines functional connectivity in the resting human brain: A simultaneous FDG-PET/fMRI study. The Journal of Neuroscience, 34(18), 6260–6266. 10.1523/JNEUROSCI.0492-14.2014. [PubMed: 24790196]

Robinson JL, Barron DS, Kirby LA, Bottenhorn KL, Hill AC, Murphy JE, et al. (2015). Neurofunctional topography of the human hippocampus. Human Brain Mapping. 10.1002/hbm.22987.

Robinson JL, Laird AR, Glahn DC, Lovallo WR, & Fox PT (2010). Metaanalytic connectivity modeling: Delineating the functional connectivity of the human amygdala. Human Brain Mapping, 31(2), 173–184. 10.1002/hbm.20854. [PubMed: 19603407]

Rottschy C, Caspers S, Roski C, Reetz K, Dogan I, Schulz JB, et al. (2013). Differentiated parietal connectivity of frontal regions for "what" and "where" memory. Brain Structure & Function, 218(6), 1551–1567. 10.1007/s00429-012-0476-4. [PubMed: 23143344]

Rottschy C, Kleiman A, Dogan I, Langner R, Mirzazade S, Kronenbuerger M, et al. (2013). Diminished activation of motor working-memory networks in Parkinson's disease. PLoS One, 8(4), e61786. 10.1371/journal.pone.0061786. [PubMed: 23620791]

Salimi-Khorshidi G, Smith SM, Keltner JR, Wager TD, & Nichols TE (2009). Meta-analysis of neuroimaging data: A comparison of image-based and coordinate-based pooling of studies. NeuroImage, 45(3), 810–823. 10.1016/j.neuroimage.2008.12.039. [PubMed: 19166944]

Schneider JS, Diamond SG, & Markham CH (1987). Parkinson's disease: Sensory and motor problems in arms and hands. Neurology, 37(6), 951–956. [PubMed: 3587646]

Seeley WW, Crawford RK, Zhou J, Miller BL, & Greicius MD (2009). Neurodegenerative diseases target large-scale human brain networks. Neuron, 62(1), 42–52. 10.1016/j.neuron.2009.03.024. [PubMed: 19376066]

Sharman M, Valabregue R, Perlbarg V, Marrakchi-Kacem L, Vidailhet M, Benali H, et al. (2013). Parkinson's disease patients show reduced cortical-subcortical sensorimotor connectivity. Movement Disorders, 28(4), 447–454. 10.1002/mds.25255. [PubMed: 23144002]

Sheng K, Fang W, Su M, Li R, Zou D, Han Y, et al. (2014). Altered spontaneous brain activity in patients with Parkinson's disease accompanied by depressive symptoms, as revealed by regional homogeneity and functional connectivity in the prefrontal-limbic system. PLoS One, 9(1), e84705. 10.1371/journal.pone.0084705. [PubMed: 24404185]

Skidmore FM, Yang M, Baxter L, von Deneen KM, Collingwood J, He G, et al. (2013). Reliability analysis of the resting state can sensitively and specifically identify the presence of Parkinson disease. NeuroImage, 75, 249–261. 10.1016/j.neuroimage.2011.06.056. [PubMed: 21924367]

Snyder AZ, & Raichle ME (2012). A brief history of the resting state: The Washington University perspective. NeuroImage, 62(2), 902–910. 10.1016/j.neuroimage.2012.01.044. [PubMed: 22266172]

Sober SJ, & Sabes PN (2005). Flexible strategies for sensory integration during motor planning. Nature Neuroscience, 8(4), 490–497. 10.1038/nn1427. [PubMed: 15793578]

Srovnalova H, Marecek R, & Rektorova I (2011). The role of the inferior frontal gyri in cognitive processing of patients with Parkinson's disease: A pilot rTMS study. Movement Disorders, 26(8), 1545–1548. 10.1002/mds.23663. [PubMed: 21480374]

Stoessl AJ (2009). Functional imaging studies of non-motoric manifestations of Parkinson's disease. Parkinsonism & Related Disorders, 15(Suppl. 3), S13–S16. 10.1016/S1353-8020(09)70771-0.

Stoessl AJ, Martin WW, McKeown MJ, & Sossi V (2011). Advances in imaging in Parkinson's disease. Lancet Neurology, 10(11), 987–1001. 10.1016/S1474-4422(11)70214-9. [PubMed: 22014434]

Szewczyk-Krolikowski K, Menke RA, Rolinski M, Duff E, Salimi-Khorshidi G, Filippini N, et al. (2014). Functional connectivity in the basal ganglia network differentiates PD patients from controls. Neurology, 83(3), 208–214. 10.1212/WNL.0000000000000592. [PubMed: 24920856]

Tahmasian M, Bettray LM, van Eimeren T, Drzezga A, Timmermann L, Eickhoff CR, et al. (2015). A systematic review on the applications of resting-state fMRI in Parkinson's disease: Does dopamine replacement therapy play a role? Cortex, 73, 80–105. 10.1016/j.cortex.2015.08.005. [PubMed: 26386442]

Tahmasian M, Knight DC, Manoliu A, Schwerthoffer D, Scherr M, Meng C, et al. (2013). Aberrant intrinsic connectivity of hippocampus and amygdala overlap in the fronto-insular and dorsomedial-prefrontal cortex in major depressive disorder. Frontiers in Human Neuroscience, 7, 639. 10.3389/fnhum.2013.00639. [PubMed: 24101900]

Tahmasian M, Pasquini L, Scherr M, Meng C, Forster S, Mulej Bratec S, et al. (2015). The lower hippocampus global connectivity, the higher its local metabolism in Alzheimer disease. Neurology, 84(19), 1956–1963. 10.1212/WNL.0000000000001575. [PubMed: 25878180]

Tahmasian M, Rochhausen L, Maier F, Williamson KL, Drzezga A, Timmermann L, et al. (2015). Impulsivity is associated with increased metabolism in the fronto-insular network in Parkinson's disease. Frontiers in Behavioral Neuroscience, 9, 317. 10.3389/fnbeh.2015.00317. [PubMed: 26648853]

Tahmasian M, Rosenzweig I, Eickhoff SB, Sepehry AA, Laird AR, Fox PT, et al. (2016 6). Structural and functional neural adaptations in obstructive sleep apnea: An activation likelihood estimation meta-analysis. Neuroscience & Biobehavioral Reviews, 65, 142–156. 10.1016/j.neubiorev.2016.03.026. [PubMed: 27039344]

Tahmasian M, Shao J, Meng C, Grimmer T, Diehl-Schmid J, Yousefi BH, et al. (2016). Based on the network degeneration hypothesis: Separating individual patients with different neurodegenerative syndromes in a preliminary hybrid PET/MR study. Journal of Nuclear Medicine, 57(3), 410–415. 10.2967/jnumed.115.165464. [PubMed: 26585059]

Talairach J, & Tournoux P (1988). Co-planar stereotaxic atlas of the human brain: 3-Dimensional proportional system: An approach to cerebral imaging. Stuttgart; New York: Georg Thieme.

Tan Y, Tan J, Deng J, Cui W, He H, Yang F, et al. (2015). Alteration of basal ganglia and right frontoparietal network in early drug-naive Parkinson's disease during heat pain stimuli and resting state. Frontiers in Human Neuroscience, 9, 467. 10.3389/fnhum.2015.00467. [PubMed: 26379530]

Tessitore A, Esposito F, Vitale C, Santangelo G, Amboni M, Russo A, et al. (2012). Default-mode network connectivity in cognitively unimpaired patients with Parkinson disease. Neurology, 79(23), 2226–2232. 10.1212/WNL.0b013e31827689d6. [PubMed: 23100395]

Tinaz S, Lauro P, Hallett M, & Horovitz SG (2015). Deficits in task-set maintenance and execution networks in Parkinson's disease. Brain Structure & Function. 10.1007/s00429-014-0981-8.

Trujillo JP, Gerrits NJ, Veltman DJ, Berendse HW, van der Werf YD, & van den Heuvel OA (2015). Reduced neural connectivity but increased task-related activity during working memory in de novo Parkinson patients. Human Brain Mapping, 36(4), 1554–1566. 10.1002/hbm.22723. [PubMed: 25598397]

Turkeltaub PE, Eden GF, Jones KM, & Zeffiro TA (2002). Meta-analysis of the functional neuroanatomy of single-word reading: Method and validation. NeuroImage, 16(3 Pt 1), 765–780. [PubMed: 12169260]

Turkeltaub PE, Eickhoff SB, Laird AR, Fox M, Wiener M, & Fox P (2012). Minimizing within-experiment and within-group effects in activation likelihood estimation meta-analyses. Human Brain Mapping, 33(1), 1–13. 10.1002/hbm.21186. [PubMed: 21305667]

Turner JA, & Laird AR (2012). The cognitive paradigm ontology: Design and application. Neuroinformatics, 10(1), 57–66. 10.1007/s12021-011-9126-x. [PubMed: 21643732]

Vervoort G, Heremans E, Bengevoord A, Strouwen C, Nackaerts E, Vandenberghe W, et al. (2016). Dual-taskrelated neural connectivity changes in patients with Parkinson' disease. Neuroscience, 317, 36–46. 10.1016/j.neuroscience.2015.12.056. [PubMed: 26762801]

Wager TD, Lindquist MA, Nichols TE, Kober H, & Van Snellenberg JX (2009). Evaluating the consistency and specificity of neuroimaging data using meta-analysis. NeuroImage, 45(1 Suppl.), S210–S221. 10.1016/j.neuroimage.2008.10.061. [PubMed: 19063980]

Wang J, Xie S, Guo X, Becker B, Fox PT, Eickhoff SB, et al. (2017). Correspondent functional topography of the human left inferior parietal lobule at rest and under task revealed using resting-state fMRI and coactivation based parcellation. Human Brain Mapping. 10.1002/hbm.23488.

Wei L, Zhang J, Long Z, Wu GR, Hu X, Zhang Y, et al. (2014). Reduced topological efficiency in cortical-basal ganglia motor network of Parkinson's disease: A resting state fMRI study. PLoS One, 9(10), e108124. 10.1371/journal.pone.0108124. [PubMed: 25279557]

Wen X, Wu X, Liu J, Li K, & Yao L (2013). Abnormal baseline brain activity in non-depressed Parkinson's disease and depressed Parkinson's disease: A resting-state functional magnetic resonance imaging study. PLoS One, 8(5), e63691. 10.1371/journal.pone.0063691. [PubMed: 23717467]

Willis AW (2013). Parkinson disease in the elderly adult. Missouri Medicine, 110(5), 406–410. [PubMed: 24279192]

Wu T, Long X, Zang Y, Wang L, Hallett M, Li K, et al. (2009). Regional homogeneity changes in patients with Parkinson's disease. Human Brain Mapping, 30(5), 1502–1510. 10.1002/hbm.20622. [PubMed: 18649351]

Wu T, Ma Y, Zheng Z, Peng S, Wu X, Eidelberg D, et al. (2015). Parkinson's disease-related spatial covariance pattern identified with resting-state functional MRI. Journal of Cerebral Blood Flow & Metabolism, 35(11), 1764–1770. 10.1038/jcbfm.2015.118. [PubMed: 26036935]

Wu T, Wang J, Wang C, Hallett M, Zang Y, Wu X, et al. (2012). Basal ganglia circuits changes in Parkinson's disease patients. Neuroscience Letters, 524(1), 55–59. 10.1016/j.neulet.2012.07.012. [PubMed: 22813979]

Yang H, Zhou XJ, Zhang MM, Zheng XN, Zhao YL, & Wang J (2013). Changes in spontaneous brain activity in early Parkinson's disease. Neuroscience Letters, 549, 24–28. 10.1016/j.neulet.2013.05.080. [PubMed: 23769726]

Yao N, Shek-Kwan Chang R, Cheung C, Pang S, Lau KK, Suckling J, et al. (2014). The default mode network is disrupted in Parkinson's disease with visual hallucinations. Human Brain Mapping, 35(11), 5658–5666. 10.1002/hbm.22577. [PubMed: 24985056]

Yuan R, Di X, Kim EH, Barik S, Rypma B, & Biswal BB (2013). Regional homogeneity of resting-state fMRI contributes to both neurovascular and task activation variations. Magnetic Resonance Imaging, 31(9), 1492–1500. 10.1016/j.mri.2013.07.005. [PubMed: 23969197]

Zhang J, Wei L, Hu X, Xie B, Zhang Y, Wu GR, et al. (2015). Akinetic-rigid and tremor-dominant Parkinson's disease patients show different patterns of intrinsic brain activity. Parkinsonism & Related Disorders, 21(1), 23–30. 10.1016/j.parkreldis.2014.10.017. [PubMed: 25465747]

Zhang J, Wei L, Hu X, Zhang Y, Zhou D, Li C, et al. (2013). Specific frequency band of amplitude low-frequency fluctuation predicts Parkinson's disease. Behavioural Brain Research, 252, 18–23. 10.1016/j.bbr.2013.05.039. [PubMed: 23727173]

Zia S, Cody FW, & O'Boyle DJ (2002). Identification of unilateral elbow-joint position is impaired by Parkinson's disease. Clinical Anatomy, 15(1), 23–31. 10.1002/ca.1087. [PubMed: 11835540]

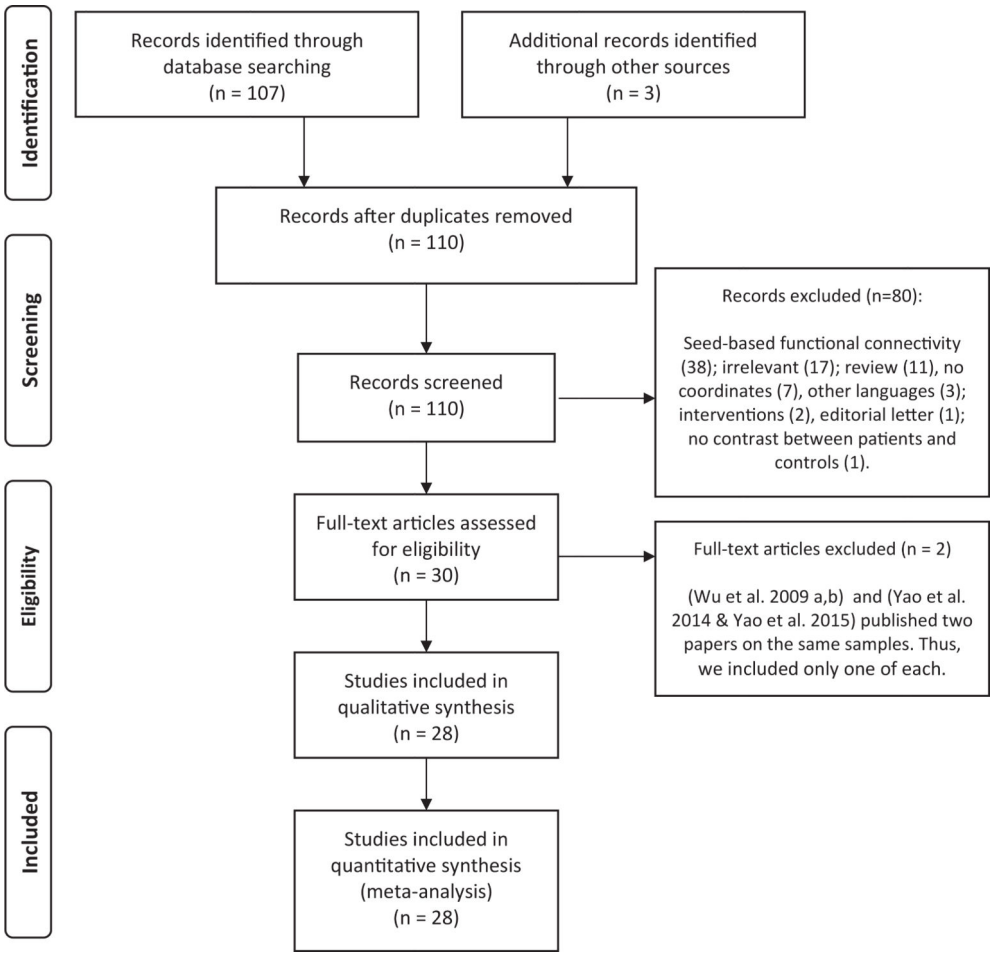

Fig. 1 –.
Paper selection strategy flow chart.

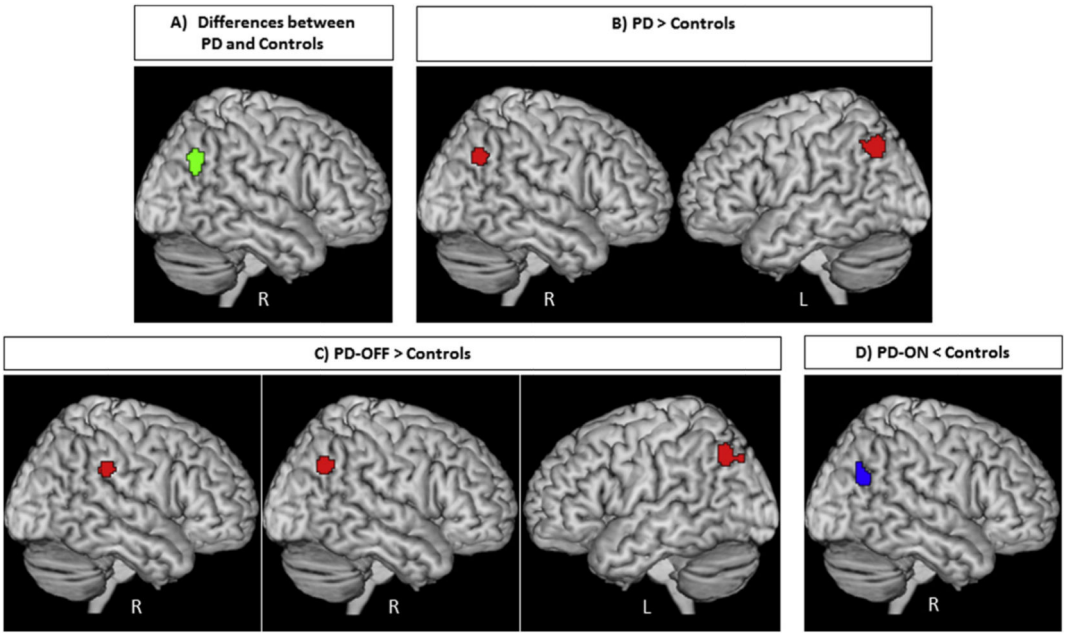

Fig. 2 –.

A) Convergence of aberrant (green) and B) convergence of increased (red) resting-state fMRI findings in patients with Parkinson's disease compared to healthy controls in bilateral parietal lobule. C) Convergence of increased (red) resting-state fMRI findings in patients with Parkinson's disease in the OFF-state compared to healthy controls in the right supramarginal gyrus and bilateral parietal lobule; D) Convergence of reduced (blue) resting-state fMRI findings in patients with Parkinson's disease in the ON-state compared to healthy controls in the right parietal lobule. All activations are significant at $p < .05$ corrected for multiple comparisons using the family-wise error rate in cluster level (cFWE).

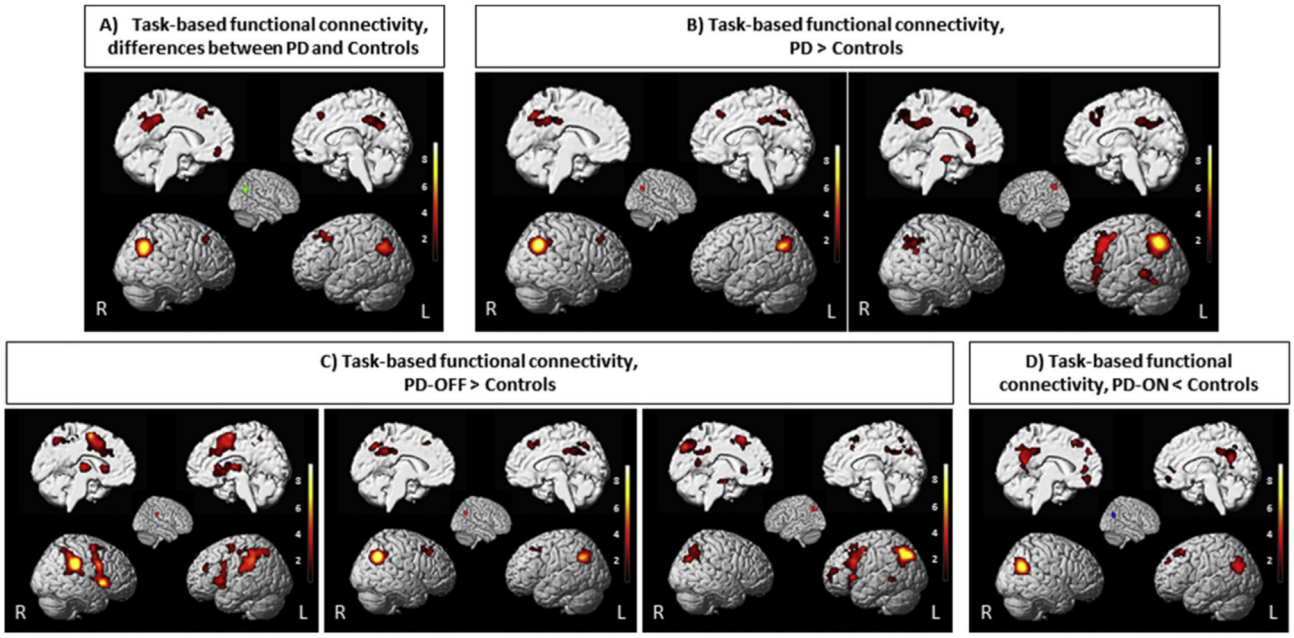

Fig. 3 –.

The results of meta-analytic connectivity modeling analysis in BrainMap data set. Task-based connectivity pattern of the seed based on ALE findings. All activations are significant at $p < .05$ corrected for multiple comparisons using the family-wise error rate in cluster level (cFWE).

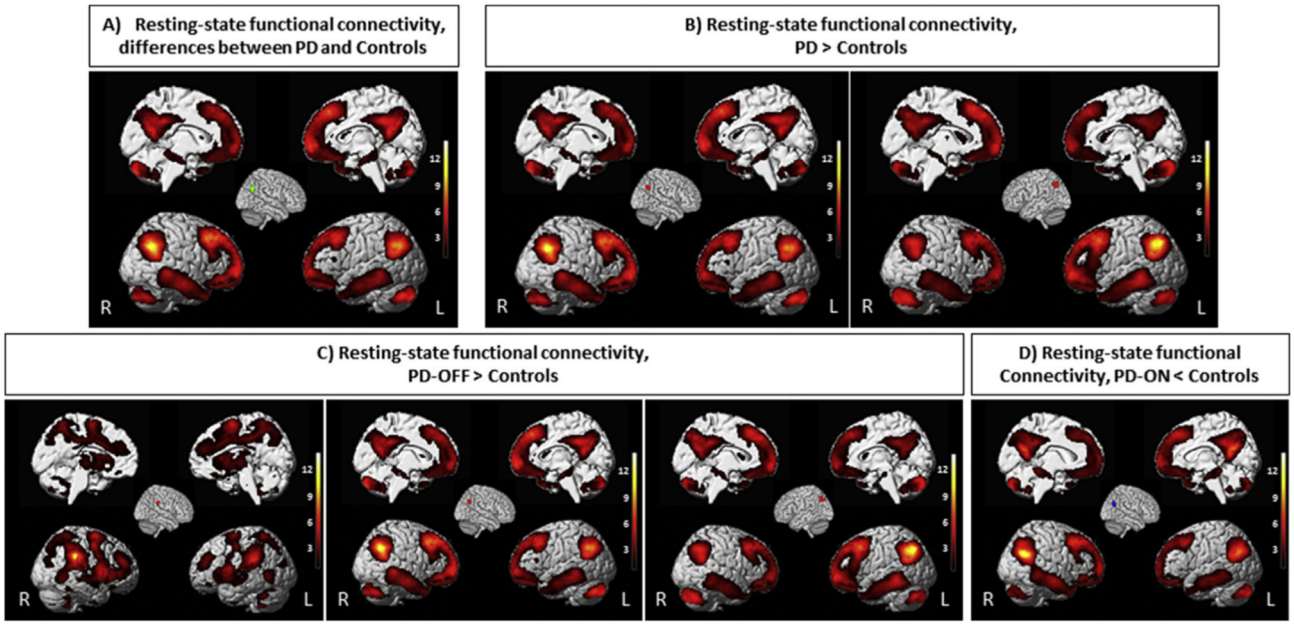

Fig. 4 –.

The results of resting-state functional connectivity in healthy participants' data set. Task-independent connectivity pattern of the seed based on ALE findings. All activations are significant at $p < .05$ corrected for multiple comparisons using the family-wise error rate in cluster level (cFWE).

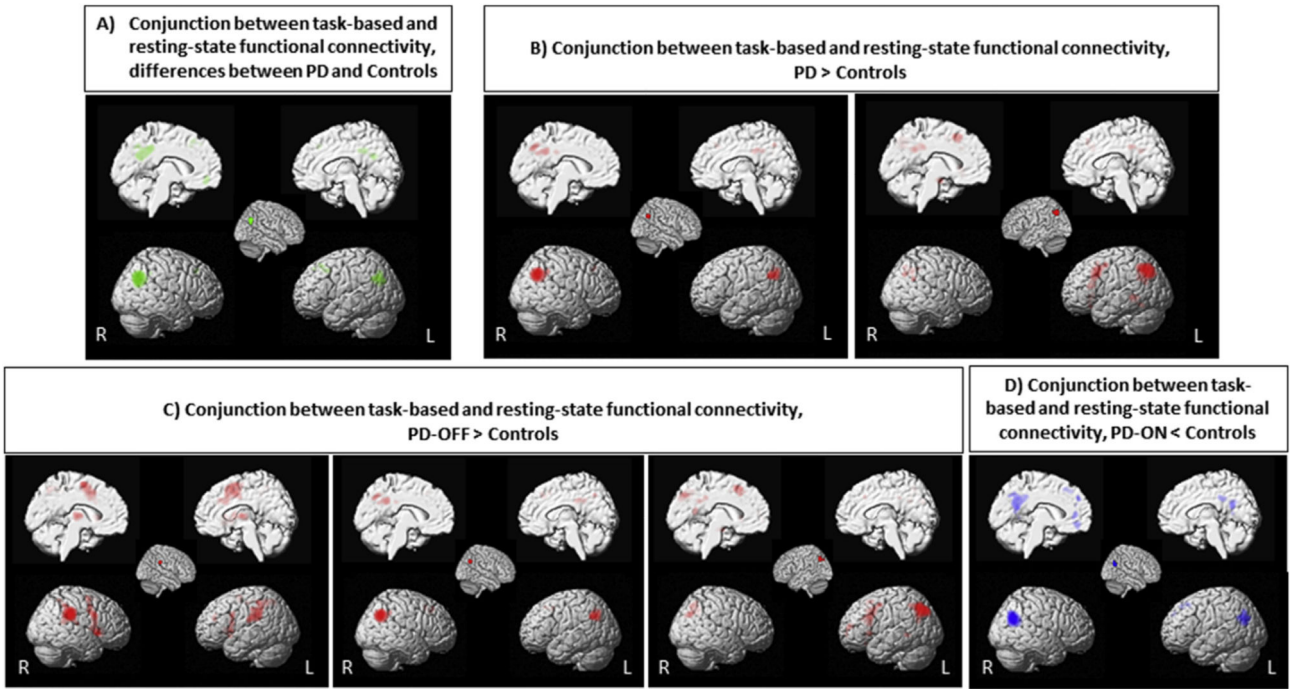

Fig. 5 –.

Conjunction analysis demonstrated regions significantly co-activated with seeds in task-based and task-independent data sets.

Table 1 –

Studies entered into the meta-analysis are listed based on the method of analysis and year of publication.

	Author, year	Number of subjects (PD/ controls)	Number of female subjects (PD/controls)	Age of PD/controls (Mean ± SD)	Imaging method	Medication status	Number of foci	Covariates	UPDRS-score
1	Chen et al. (2015)	31 (12 TD, 19 PIGD)/22	15 (8 TD, 7 PIGD)/10	62.6 ± 8.71 (TD), 64.8 ± 8.34 (PIGD)/65.1 ± 5.00	ALFF	ON	12	Age, gender, Levodopa equivalent daily dosage, grey matter volume	TD: Part III: 19.1 ± 11.5 PIGD: Part III: 21.6 ± 11.6
2	Hu et al. (2015)	17/20	7/9	60.29 ± 12.03/58.48 ± 6.89	ALFF	ON	3	Mean FD	Baseline: Part III: 17.11 ± 6.12 Follow-up: Part III: 17.29 ± 6.30
3	Wu et al. (2015)	58/54	25/26	61.4 ± 9.0/61.1 ± 9.4/	ALFF	OFF	31	N/S	Part III (OFF): 24.8 ± 8.2
4	Yao et al. (2014)	24 (12 PD_nonVH, 12 PD_VH)/14	17 (8 PD_nonVH, 9 PD_VH)/8	63.4 ± 7.4 (PD_nonVH), 67.6 ± 7.4 (PD_VH)/64.1 ± 4.0	ALFF	ON	12	Depression scores	PD_nonVH: Part III: 18 ± 12.9 PD_VH: Part III: 20.9 ± 10.6
5	Hou et al. (2014)	109/106	42/42	59.84 ± 7.15/59.91 ± 7.09	ALFF	OFF	23	N/S	Part III (OFF): 25.54 ± 11.51
6	Luo et al. (2014)	59 (29 PD_D, 30 PD_nonD)/30	30 (15 PD_D, 15 PD_nonD)/15	51.46 ± 8.21 (PD_D) 53.64 ± 10.18 (PD_nonD)/51.9 ± 7.70	ALFF	Drug naive	1	Age, gender	PD_D (naïve): Part I: 3.69 ± 2.00 Part II: 9.93 ± 6.69 Part III: 28.34 ± 16.9 Part IV: 0 PD-nonD (naïve): Part I: 1.23 ± 1.33 Part II: 8.40 ± 4.44 Part III: 26.83 ± 12.44 Part IV: 0
7	Skidmore et al. (2013)	14/15	3/6	62 ± 9/65 ± 13	ALFF	OFF	8	Head motion	OFF: Part I: 4 ± 3 Part II: 12 ± 8 Part III: 37 ± 13 Part VI: 3 ± 2 TOTAL: 56 ± 23
8	Wen et al. (2013)	33 (17 PD_D, 16 PD_nonD)/21	26 (10 PD_D, 8 PD_nonD)/8	64.4 ± 13.4 (PD_D), 60.7 ± 18.7 (PD_nonD)/55.4 ± 16.4	ALFF	OFF	36	N/S	Probably Total Score: PD_D (OFF): 42 ± 46 PD_nonD (OFF): 33.8 ± 24.2
9	Zhang et al. (2013)	72/78	47/46	59.7 ± 11.9/58.6 ± 8.5	ALFF	OFF	18	Age, gender, mean grey matter volumes, mean relative FD	Part III (OFF): 20.24 ± 8.44
10	Kwak et al. (2012)	24/24	2/5	64 ± 8/63 ± 7	ALFF	ON versus OFF	35	N/S	Part III (ON): 17.3 ± 8 Part III (OFF): 18.5 ± 8

	Author, year	Number of subjects (PD/ controls)	Number of female subjects (PD/controls)	Age of PD/controls (Mean ± SD)	Imaging method	Medication status	Number of foci	Covariates	UPDRS-score
11	Borroni et al. (2015)	21 (11 PD, 10 PD_CI)/10	13 (1 PD, 4 PD_CI)/7	66.3 ± 3.8 (PD), 74.5 ± 4.6 (PD_CI),/62.2 ± 8.0	ReHo	N/S	4	VBM	PD: Part III: 10.7 ± 5.4 PD_CI: Part III: 27.9 ± 10.5
12	Zhang et al. (2015)	47 (27 AR, 20 TD),/26	21 (11 AR, 10 TD)/15	63.38 ± 9.46 (AR), 54.55 ± 12.58 (TD)/59.31 ± 7.15	ReHo	OFF	58	Gender, age, mean grey matter volumes, mean relative FD	AR: Part III (OFF): 19.88 ± 6.70 TD: Part III (OFF): 19.35 ± 9.35
13	Sheng et al. (2014)	41 (20 PD_D, 21 PD_nonD)/25	15 (8 PD_D, 7 PD_nD)/9	55.9 ± 7.4 (PD_D) 57.3 ± 6.1(PD_nonD)/56.7 ± 5.3	ReHo	OFF	12	N/S	PD_D: Part III (OFF): 39.4 ± 10.8 PD_nonD: Part III (OFF): 43.8 ± 8.2
14	Choe et al. (2013)	22/25	12/15	58.3 ± 2.4/58.3 ± 1.7	ReHo	OFF	11	N/S	Part III (OFF): 10.4 ± 1.2
15	Yang et al. (2013)	17/17	7/7	60.43 ± 9.65/60.73 ± 8.57	ReHo	OFF	17	N/S	Part III (OFF): 20.57 ± 3.82
16	Wu et al. (2009)	22/22	6/N/S	59.5 ± 8.1/59.7 ± N/S	ReHo	ON versus OFF	39	N/S	OFF: 25.6 ± 8.1
17	Tinaz et al. (2015)	30/30	11/10	61.2 ± 8.4/61.4 ± 6.7	Graph	OFF	21	N/S	Part III (OFF): 28.4 ± 11.7 TOTAL (OFF): 46.5 ± 15.2
18	Wei et al. (2014)	37/34	20/12	58.68 ± 13.10/55.59 ± 10.55	Graph	OFF	12	age, gender and mean FD	Part III (OFF): 19.17 ± 9.22
19	Gottlich et al. (2013)	37/20	15/10	65 ± 10/63 ± 9	Graph	ON	10	N/S	Part III (ON): 22.3 ± 7.7
20	Baggio et al. (2014)	65 (22 PD_CI, 43 PD_nonCI)/36	42 (8 PD_CI, 20 PD_nonCI)/17	66.1 ± 12.2 (PD_CI), 64.0 ± 9.8 (PD_nonCI)/63.4 ± 10.5	Network	ON	5	Head motion	PD_CI: Part III (ON): 18.2 ± 8.7 PD_nonCI: Part III (ON): 14.1 ± 7.5
21	Gorges et al. (2015)[a]	31 (17 PD_CI, 14 PD_ nonCI)/22	12 (9 PD_CI, 3 PD_ nonCI)/7	69 ± 8 years PD-CI), 67 ± 10 (PD_ nonCI)/68 ± 6 years	Network	ON	68	N/S	PD_all: Part III (ON): 12 (8–14) PD_CI: Part III (ON): 12 (9–18) PD_nonCI: Part III (ON): 10 (5–13)
22	Madhyastha et al. (2015)	24/21	7/12	66.08 ± 10.27/61.90 ± 10	Network	ON	4	N/S	Part I: 9.78 ± 5.81 Part II: 8.38 ± 5.08 Part III: 23.12 ± 8.61 Part IV: 1.88 ± 3.72
23	Onu et al. (2015)	27/16	N/S	68.7 ± 10.6/67 ± 11.5	Network	OFF	35	N/S	Part III (OFF): 28.4 ± 9.5 Part III (ON): 9.2 ± 5.2
24	Tan et al. (2015)	14/17	3/4	62.79 ± 4.59/61.35 ± 4.27	Network	Drug naive	6	N/S	Naïve: Part I: 2.93 ± 1.14 Part II: 9.93 ± 2.27

	Author, year	Number of subjects (PD/ controls)	Number of female subjects (PD/controls)	Age of PD/controls (Mean ± SD)	Imaging method	Medication status	Number of foci	Covariates	UPDRS-score
									Part III: 21.79 ± 5.66 Part VI: 0
25	Szewczyk-Krolikowski et al. (2014)	19/19	9/8	58.9 ± 10.8/60.6 ± 7.7	Network	ON versus OFF	14	N/S	Discovery: Part III: 23.9 ± 9.6 Validation: Part III: 29.7 ± 14.7
26	Amboni et al. (2014)	42 (21 PD_CI, 21 PD_nonCI)/20	10 (3 PD_CI, 7 PD_nonCI)/8	65.2 ± 8.7 (PD_CI), 65.8 ± 6.5 (PD_nonCI)/61.9 ± 9.2	Network	ON	8	Total intracranial volume, age and gender	PD_CI: Part III (ON): 14.3 ± 8.5 PD_nonCI: Part III (ON): 13.1 ± 5.3
27	Esposito et al. (2013)	20 (10 levodopa, 10 placebo)/18	10 (5 levodopa, 5 placebo)/8	60.8 ± 8.66 (levodopa), 66.7 ± 5.29 (placebo)/59.2 ± 1.52	Network	ON versus OFF	3	N/S	Levodopa: Part III (OFF): 16.3 ± 3.91 Part III (ON): 10.7 ± 3.19 Placebo: Part III (OFF): 20.5 ± 7.09 Part III (ON): 19.8 ± 7.88
28	Tessitore et al. (2012)	16/16	4/4	64.15 ± 1.64/65.5 ± 6.17	Network	ON	2	Total intracranial volume and age	Part III (ON): 11.50 ± .97

ALFF = amplitude of low frequency fluctuation; FD = frame-wise displacement; PD = Parkinson's disease; PD_CI = Parkinson patients with cognitive impairment; PD_nonCI = Parkinson patients without cognitive impairment; PD_D = Parkinson patients with depression; PD_nonD = Parkinson patients without depression; PD_VH = Parkinson patients with visual hallucinations; PD_nonVH = Parkinson patients without hallucinations; PIGD = postural instability/gait difficulty; ReHo = regional homogeneity; TD = tremor-dominant; UPDRS = Unified Parkinson's Disease Rating Scale (Part I = non-motor aspects of experiences of daily living, Part II = motor aspects of experiences of daily living, Part III = motor examination, Part IV = motor complications); VBM = voxel-based morphometry.

[a]Data are given as median (interquartile range).